AD-A099 264 RESEARCH TRIANGLE INST RESEARCH TRIANGLE PARK NC F/G 8/3
QUASI REALTIME OCEANOGRAPHIC EXPERIMENT USING NOAA SATELLITE DA--ETC(U)
FEB 75 F M VUKOVICH NOAA-3-35402

UNCLASSIFIED NL

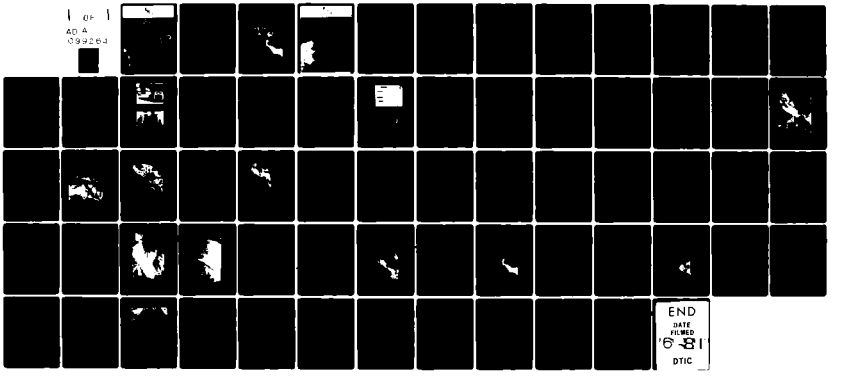

RESEARCH TRIANGLE INSTITUTE

LEVEL II

QUASI REALTIME OCEANOGRAPHIC EXPERIMENT USING NOAA SATELLITE DATA AND SHIP DATA

Fred M. Vukovich
Research Triangle Institute

February 1975

FINAL REPORT

Contract No. 3-35402

Prepared for

National Environmental Satellite Service
National Oceanic and Atmospheric Administration
Washington, D. C.

By

The Research Triangle Institute
Research Triangle Park, N. C. 27709

ERRATA

P. 17, first paragraph, third line. The sentence should read "South of the eddy in Onslow Bay and east of Cape Romain, a tongue of shelf water is shown intruding into the Gulf Stream".

P. 20, last paragraph, sixth line. "36.2 °/₀₀" should be "36.3 °/₀₀".

P. 23, caption to Figure 3.1.3.9 should read: "High resolution temperature (°C) analysis of the first 20 meters along the track marked I. Station numbers are given at the top of the figure".

P. 35, first paragraph, seventh line. "obtianed" should be "obtained".

P. 42, caption to Figure 3.2.3.1, first line. "periods" should be "period".

P. 43, fourth paragraph, first line. "made up a" should be "made up of a".

P. 46, first paragraph, fourth line, "Figure 3.2.2.1" should be "Figure 3.2.2.2".

P. 46, seventh line, "Figure 3.2.2.1" should be "Figure 3.2.2.3".

P. 46, last paragraph, second line, "Transect II" should be "Transect III".

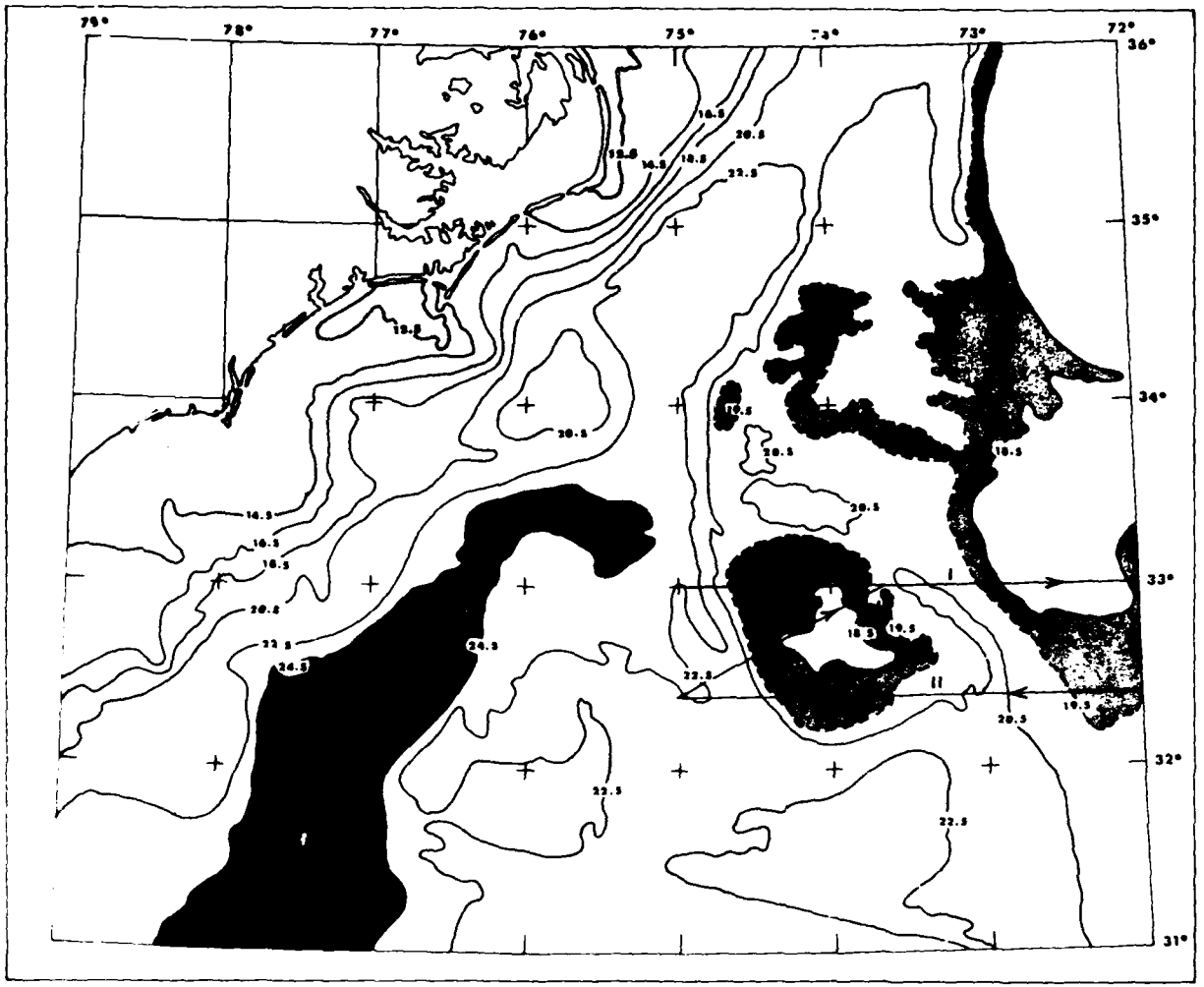

Figure 3.2.2.3 Sea-surface temperature analysis (°C) using digitized NOAA-3 VHRR data for 1 April 1974. Transects I, II and III are also indicated.

RESEARCH TRIANGLE INSTITUTE

(15) NOAA-3-35402

Ordered 2/25/80

(6)

QUASI REALTIME OCEANOGRAPHIC EXPERIMENT USING NOAA SATELLITE DATA AND SHIP DATA.

NA

(10) Fred M. Vukovich
Research Triangle Institute

(12) 64

(11) February 1975

(9) FINAL REPORT.

Contract No. 3-35402

Prepared for

National Environmental Satellite Service
National Oceanic and Atmospheric Administration
Washington, D. C.

By

The Research Triangle Institute
Research Triangle Park, N. C. 27709

304400

ACKNOWLEDGEMENTS

The author wishes to acknowledge the interest and assistance of Dr. E. P. McClain, Dr. P. K. Rao, Dr. A. E. Strong, and Mr. John Pritchard, all of NOAA/NESS. The author wishes also to express his appreciation to Captain Arthur Jordan, his staff, and the crew of the Cape Fear Technical Institute's (CFTI), R/V ADVANCE II and R/V DALLAS HERRING. The author was assisted in the operation of the RTI ground station and in a portion of the data analysis by Mr. B. Crissman. The author wishes to thank the numerous members of the NOAA weather station at the Raleigh-Durham Airport for their assistance in providing weather reports and collecting the orbit data for the NOAA satellites, and Mr. John McFall and Mr. James Usury, NASA/Langley Research Center, for the use of and for their assistance with the EOLE buoy.

ABSTRACT

A series of oceanographic studies was performed off the southeast coast of the United States, combining data from the NOAA-2 and NOAA-3 satellite and from the Cape Fear Technical Institute, R/V DALLAS HERRING and R/V ADVANCE II. The phenomena studied consisted of short-period intrusions of shelf water into the Gulf Stream and a cold eddy on the east side of the Gulf Stream. The satellite data were used to identify and locate these perturbations in realtime, and to define the sea-surface temperature distribution associated with the perturbations. The location data obtained from the satellite imagery were used to plan an oceanic field program using a ship to collect temperature and salinity data in the perturbation. The integration of satellite data with in-situ data yielded some rather interesting aspects of the physical structure of both phenomena studied. The most significant contribution of the satellite data was the capability of these data to provide an instantaneous, near-synoptic view of the sea-surface temperature pattern that brought to light factors that could have never been identified by the in-situ data alone.

TABLE OF CONTENTS

LIST OF FIGURES

LIST OF TABLES

SECTION 1.0

INTRODUCTION

Recent improvements in data transmission from environmental satellites have resulted in the acquisition of relatively noise-free infrared radiation (IR) data representative of the temperature distribution on the earth's surface in a cloud-free environment. These data are extremely useful in determining the surface temperature distribution in the ocean (Rao et al., 1971; Smith et al., 1970; Vukovich, 1971; Maul and Hansen, 1972; and Vukovich, 1974). It is now feasible to consider integration of the satellite IR data with conventional oceanographic data in a meaningful way.

One of the major contributions that satellite IR data offers is an instantaneous, quasi-realtime view of the sea-surface temperature distribution. These data can be used to study the day-to-day behavior of the ocean in terms of the surface manifestations of that behavior, and to detect and locate oceanic eddies that have associated surface temperature perturbations. These data may be used to direct the oceanographer to significant ocean features whereby in-situ data may be obtained for detailed analysis of ocean behavior. In essence, this constitutes quasi-realtime oceanography to the extent that the oceanographer will have immediate knowledge (location, character, scale, etc.) of the oceanic phenomena.

In the spring of 1973 and 1974, the Research Triangle Institute (RTI) conducted several realtime oceanic studies off the North Carolina coast. Infrared data from the NOAA-2 and NOAA-3 satellites were used to detect and locate oceanic eddies. Satellite data were obtained from a satellite receiving station on the campus of the Institute. When ocean features of interest were detected, a ship from the Cape Fear Technical Institute (CFTI) was dispatched into the region of interest to collect in-situ data. Afterwards digitized satellite data were integrated with the in-situ data to yield a physical description of the ocean feature. This report describes the results of analysis of data from the two study periods.

SECTION 2.0

SATELLITE DATA AND SHIP DATA

2.1 NOAA Satellite Data

NOAA-2 and NOAA-3 data were used for these studies. These satellites were equipped with two (2) radiometers capable of detecting radiation from the earth's surface. The SR (Scanning Radiometer) detects radiation on the 10.0 to 12.5 μm infrared, water vapor window band. Some aspects of the absorption characteristics of this band have been discussed by Vukovich (1972). The surface resolution of this radiometer was approximately 7.5 km at zero (0°) nadir angle and at the satellite's designed altitude of approximately 1500 km. The IR data were transmitted to the ground stations as an analog signal in one of two modes. Most of the data collected during one orbit were stored on tape recorders aboard the satellite and were transmitted at some later time when the satellite was in range of a ground acquisition station. These data were digitized, converted into equivalent blackbody temperatures, and rectified on the earth.

In some instances, the SR data were read out directly without being stored on the tape recorder. Data were available in this form only when the satellite is in range of a ground station. These data are called the DRIR (Direct Read-Out Infrared) data. These data, too, were digitized and converted into equivalent blackbody temperatures; but, since ephemeris data are not available for the DRIR, rectification of data was subjective and was based on available landmarks.

The other radiometer from which IR data were available, was the VHRR (Very High Resolution Radiometer). The VHRR detected IR radiation in the same water vapor window band as did the SR. The main difference between the two radiometers was the resolution parameter. The ground resolution for the VHRR was 0.9 km at zero (0°C) nadir angle and at 1500 km. The data were mainly transmitted directly to a ground station, but at a different frequency than that used for the DRIR data.

For this study, the VHRR data were used in the analysis of the various oceanic phenomena because of the superior resolution. However,

since DRIR data were received by a ground station at RTI, these data were used to detect and locate the oceanic features so that a ship could be dispatched into the region to collect in-situ data.

2.2 The RTI Receiving Station

The basic components of the RTI receiving station are shown in Figure 2.1.1.1. In the center of the figure is the EMR Model 111 AD weather satellite photo receiver. The photo receiver is made up of two basic units: an FM receiver and an oscilloscope display unit. The FM receiver can receive signals in the following frequencies: 135.60 mHz, 136.95 mHz, 137.50 mHz, and 137.62 mHz. The first two frequencies are principally used by the ATS satellites; the third by the NOAA satellites; and the last by the earlier ESSA satellites.

The oscilloscope device yields a scan line by scan line display of the IR data with a limiting resolution of 600 lines per photograph. Picture synchronization is attained automatically from the signal format data. The beam on the oscilloscope is intensity modulated, permitting more than twelve shades of gray to be distinguished on the photograph. The photograph of the line-by-line display is taken by a Polaroid camera through time exposure photography.

To the right of the receiver is the DRIR adapter that controls the vertical and horizontal sweep rate of the oscilloscope in order to conform with the signal received from the NOAA satellite. Integrated with the adapter is a linearization unit that produces a systematic non-linear horizontal sweep on the oscilloscope. This has the effect of eliminating the distortion produced by the earth's curvature and all distances on the photographic display become linear. Located atop the DRIR adapter in the figure are the azimuth and elevation controls for the antenna.

To the left of the receiver is a standard stereophonic tape recorder used to record the DRIR data when received. The data are recorded and played back simultaneously on two channels. This is done to reduce signal dropout due to impurities on the tape. Not shown in the figure is the video remodulation unit designed for insertion between the tape playback unit and the photo receiver. The unit has a non-linear transfer function that can be used to enhance the intensity of the whites or blacks of the pictures.

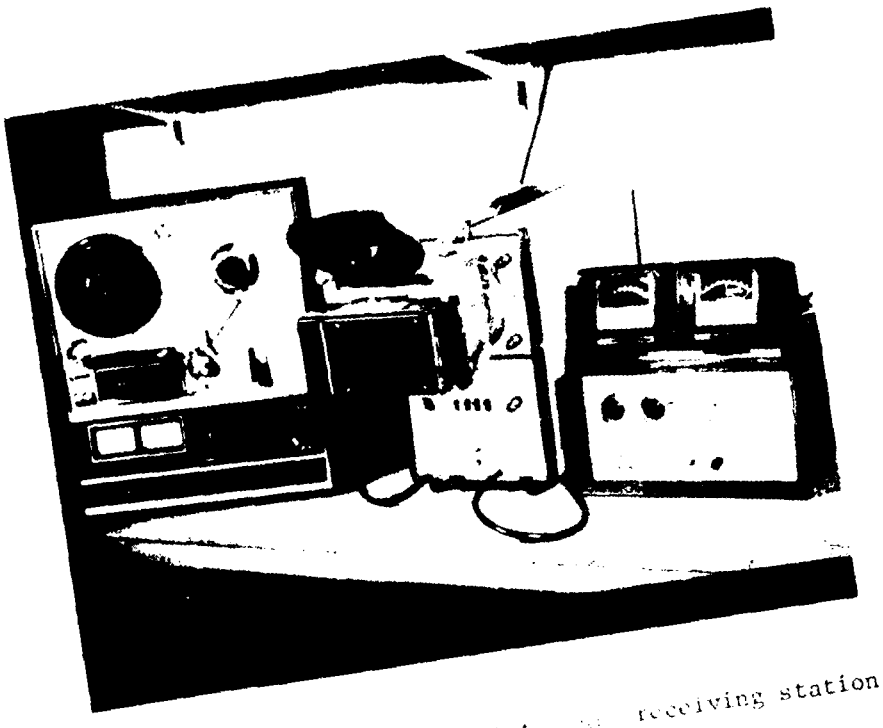

Figure 2.1.1.1 Components of [illegible] receiving station.

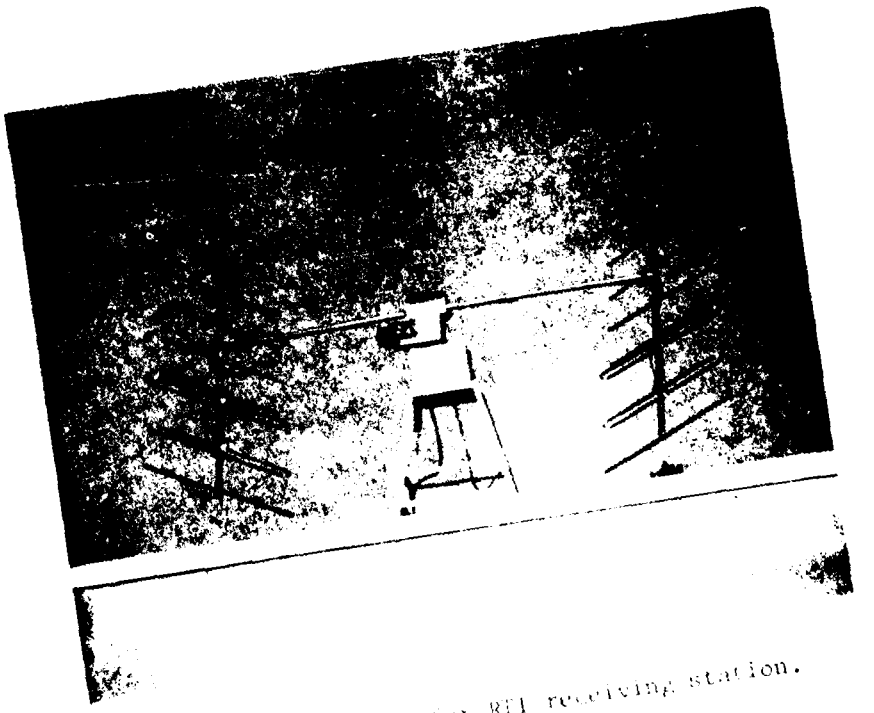

Figure 2.1.1.2 Antenna for REI receiving station.

Figure 2.1.1.2 shows the double rotator antenna used to track spacecraft. The antenna consists of two plane-wave yagi antennas which are affixed to the ends of an eight-foot boom extended from the upper gear housing. The antenna positioning is achieved by manual operation of the remote control units shown in Figure 2.1.1.1. For each orbit, precise minute-by-minute elevation and azimuth values may be determined from data distributed by NOAA.

2.3 Ship Data

When an ocean feature was detected using the DRIR data, a CFTI ship was dispatched from Wilmington, North Carolina into the region of interest to collect surface and subsurface data. For the spring 1973 case studies, the R/V DALLAS HERRING was used; and for the spring 1974, the R/V ADVANCE II was employed. Surface temperature was obtained by towing a thermistor. Subsurface temperature and salinity were determined using an STD at stations along transects specified through analysis of the DRIR photographic displays. Subsurface data were obtained down to the 500-m level or the bottom, whichever came first. Calibrations of the towed thermistor and the STD were performed before and after each study period.

SECTION 3

OCEANOGRAPHIC STUDIES

3.1 Short-Term Cold Water Intrusions into the Gulf Stream

3.1.1 General

During the period 1 May to 15 June 1973, an intensified surveillance of the behavior of the Gulf Stream off the southeast coast of the United States was carried out using infrared photographs obtained from radiometer aboard the NOAA-2 satellite. The data from the SR revealed the temperature pattern of the surface water in the region of interest. On two occasions during the period (6 May 1973 and 21 May 1974) eddies of seemingly a similar nature and from initial indication, thought to be identical to those observed by DeRycke and Rao (1973) and Rao et al. (1971), were detected.

3.1.2 Case Study: 5-8 May 1973

During this period, the general meteorological conditions were as follows. A high pressure system centered in the Midwest on 5 May 1973 governed the synoptic weather situation off the southeast coast of the United States until the approach of a low pressure system late in the day on 7 May 1973. The winds were generally from the north until 1800 EST on 7 May (Figure 3.1.2.1). The period of north winds was characterized by large fluctuations of wind speed with intervals of wind speed as high as 15 ms^{-1} and periods of very low wind speeds.

Figure 3.1.2.2a is a VHRR infrared photograph obtained from NOAA-2 at 2100 EST on 6 May. A graphical interpretation of the figure is given in Figure 3.1.2.2b. The region of interest is the area between Cape Hatteras and Cape Lookout (Raleigh Bay). The photograph shows cold, shelf water along the coast with a broad extension east of Cape Lookout that turns northward in the form of a narrow filament. This filament seemingly cuts off a lens of Gulf Stream water from the main body of the Gulf Stream in Raleigh Bay.

On the morning of 7 May, the R/V DALLAS HERRING was dispatched into the area and reached the first station of the transect depicted in

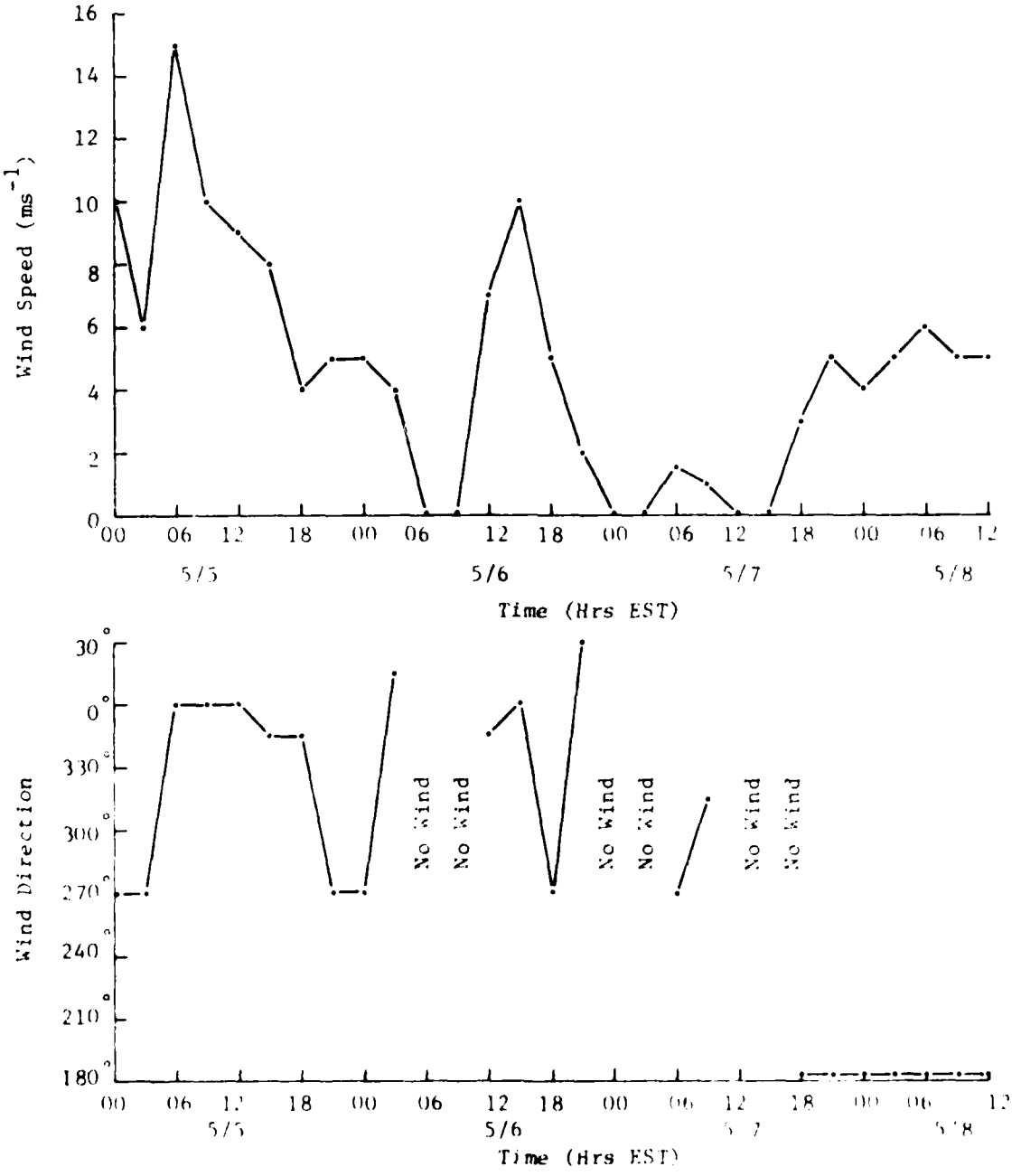

Figure 3.1.2.1 Three-hourly wind data for Diamond Shoals Light Station (35.2°N and 75.3°W).

A

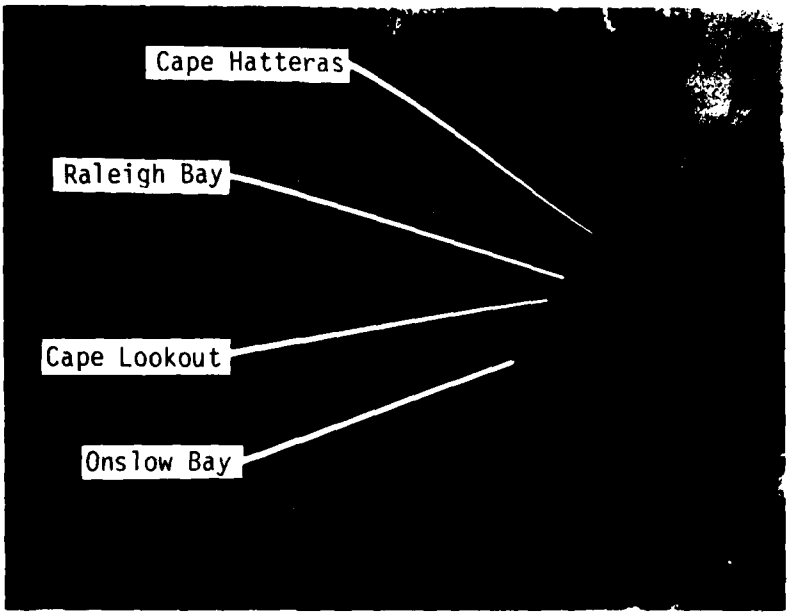

B

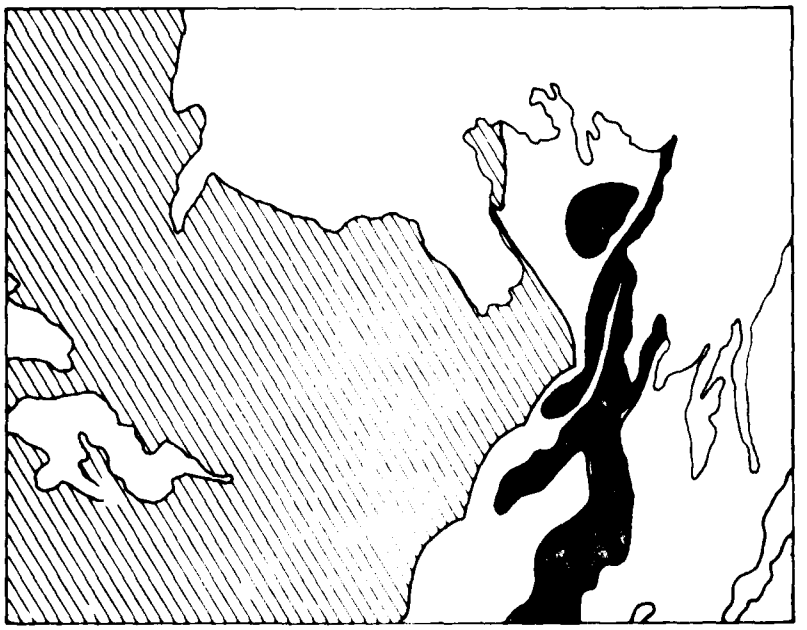

Figure 3.1.2.2 a) NOAA-2 VHRR infrared photograph for 6 May 1973 at 2100 EST.
b) Graphical interpretation of the VHRR photograph in 3a. Slanted lines indicate land mass; white indicates clouds; light gray indicates cold shelf water, and dark gray is warm Gulf Stream water.

Figure 3.1.2.3 early on 8 May. The transect disects the cold water off Cape Lookout shown in Figure 3.1.2.2. The subsurface temperature and salinity analysis from the section (Figures 3.1.2.4 and 3.1.2.5) shows a cold, relatively fresh water mass located on the north side of the Cape Lookout Shoals (Station 5). There is a strong temperature gradient, as well as salinity gradient between Stations 5 and 6, extending from the surface to the bottom. This factor and the narrowness of the cold water mass gives the impression that the mass is being pressed up against the shoals. The warm water at Station 7 is apparently the cut-off lens of Gulf Stream water.

The orientation of the shelf water in the satellite photograph and the surface weather data suggest that current within the shelf water is most probably southward along the coast, eastward in the cold water just east of Cape Lookout, and northward in the filament further east of Cape Lookout. This is somewhat fortified by computations of geostrophic current using the data from Figures 3.1.2.4 and 3.1.2.5. Figure 3.1.2.6, the analysis of geostrophic current, shows that the current in the cold, relatively fresh water on the north side of the Cape Lookout Shoals is eastward in direction (i.e., the region of positive values of the geostrophic current depicts a region where the transport is generally eastward). However, these data must be considered only a rough approximation to the actual current in that region.

If the currents in Raleigh Bay suggested by the orientation of the shelf water in Figure 3.1.2.2 are correct, one could conclude that the southwestward currents along the coast encounter the shoals which act as a barrier to the flow and the shelf water is turned eastward. The transfer of momentum and mass northward farther east of Cape Lookout must be due to shelf water penetration into the Gulf Stream.

3.1.3 Case Study: 20-23 May 1973

A slow-moving cold front approached the southeast coast on 20 May and frontal passage occurred along the coast at approximately 0300 EST on 22 May. Winds were extremely light on 20 May and 23 May. However, just prior to the passage of the front, strong southwesterly flow (on the average 13 ms^{-1}) was established, lasting about nine hours (Figure 3.1.3.1). After the front passed and the flow was from the northwest, the wind speed decreased.

On 21 May 1973, a significant temperature perturbation was detected in Onslow Bay (34°N, 76.8°W) (Figure 3.1.3.2 ... a VHRR infrared image).

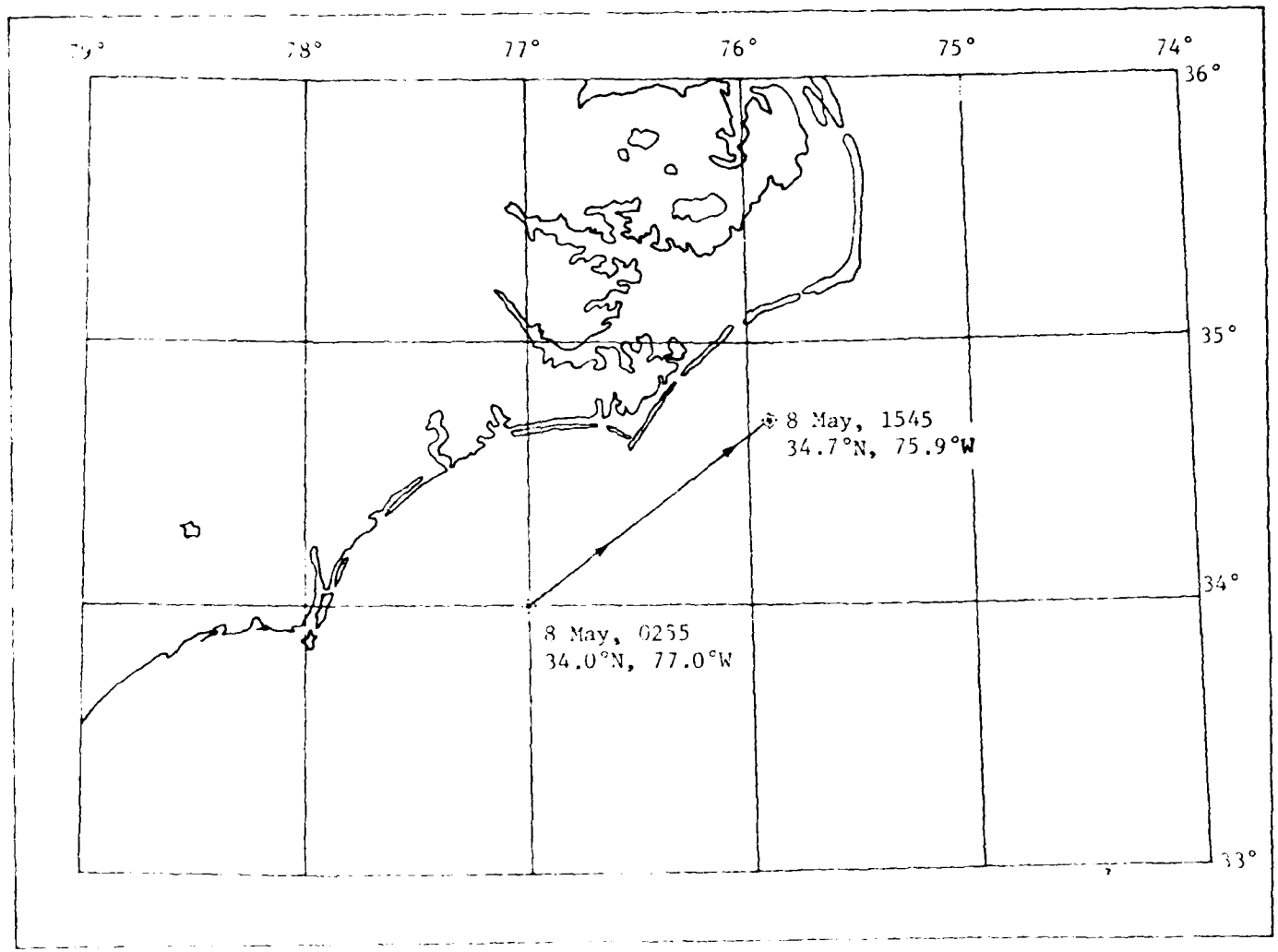

Figure 3.1.2.3 Track of the R/V DALLAS HERRING between 0255 and 1545 EST on 8 May 1973.

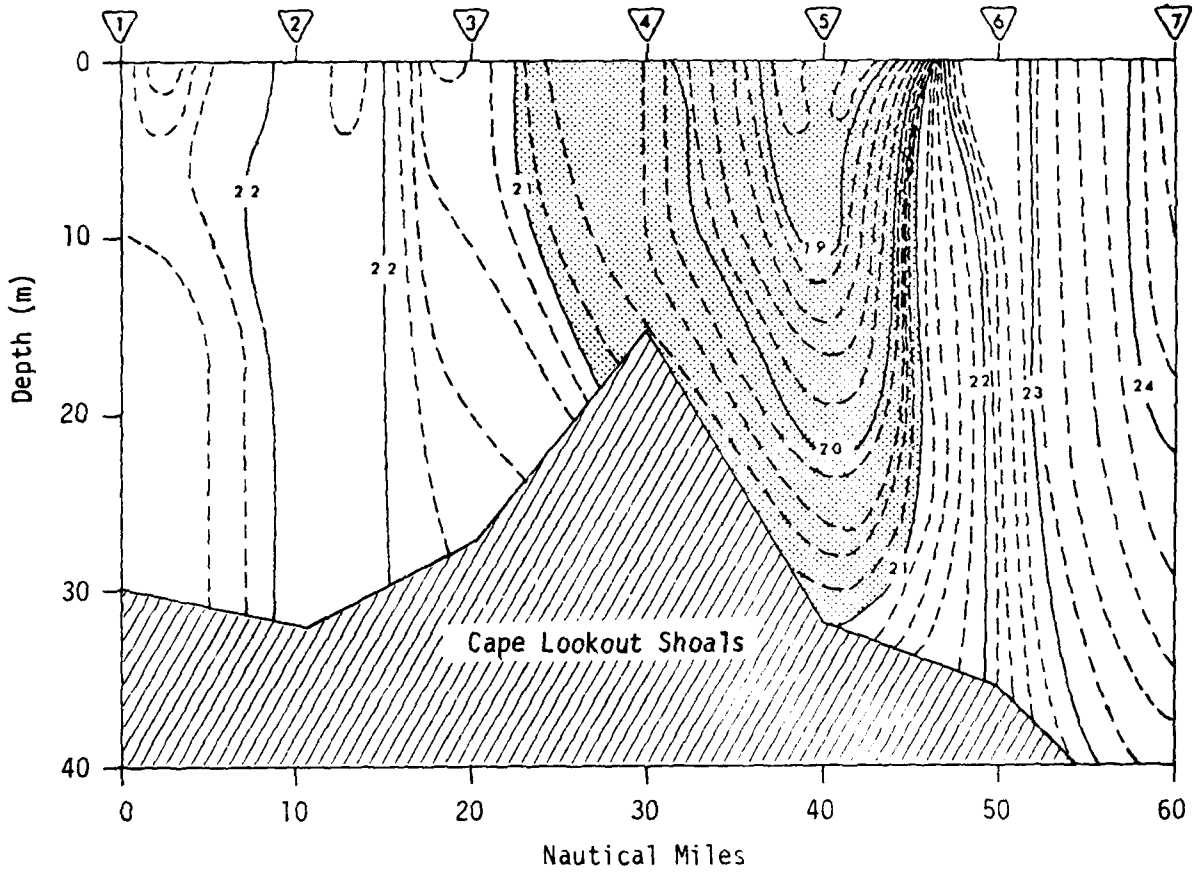

Figure 3.1.2.4 Vertical temperature (°C) cross-section from data collected by the R/V DALLAS HERRING. Station numbers are given in triangles at the top of the figure.

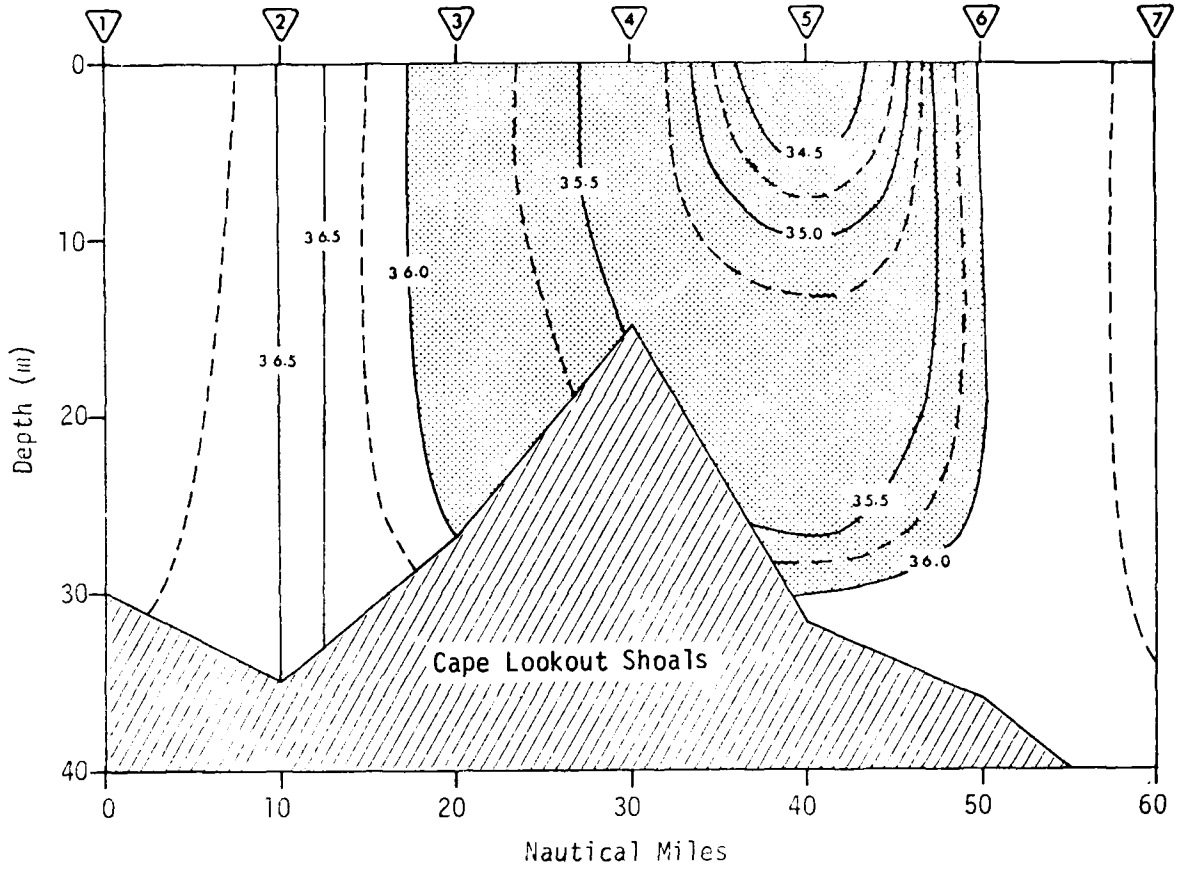

Figure 3.1.2.5 Vertical salinity (°/₀₀) cross-section from data collected by the R/V DALLAS HERRING. Station numbers are given in triangles at the top of the figure.

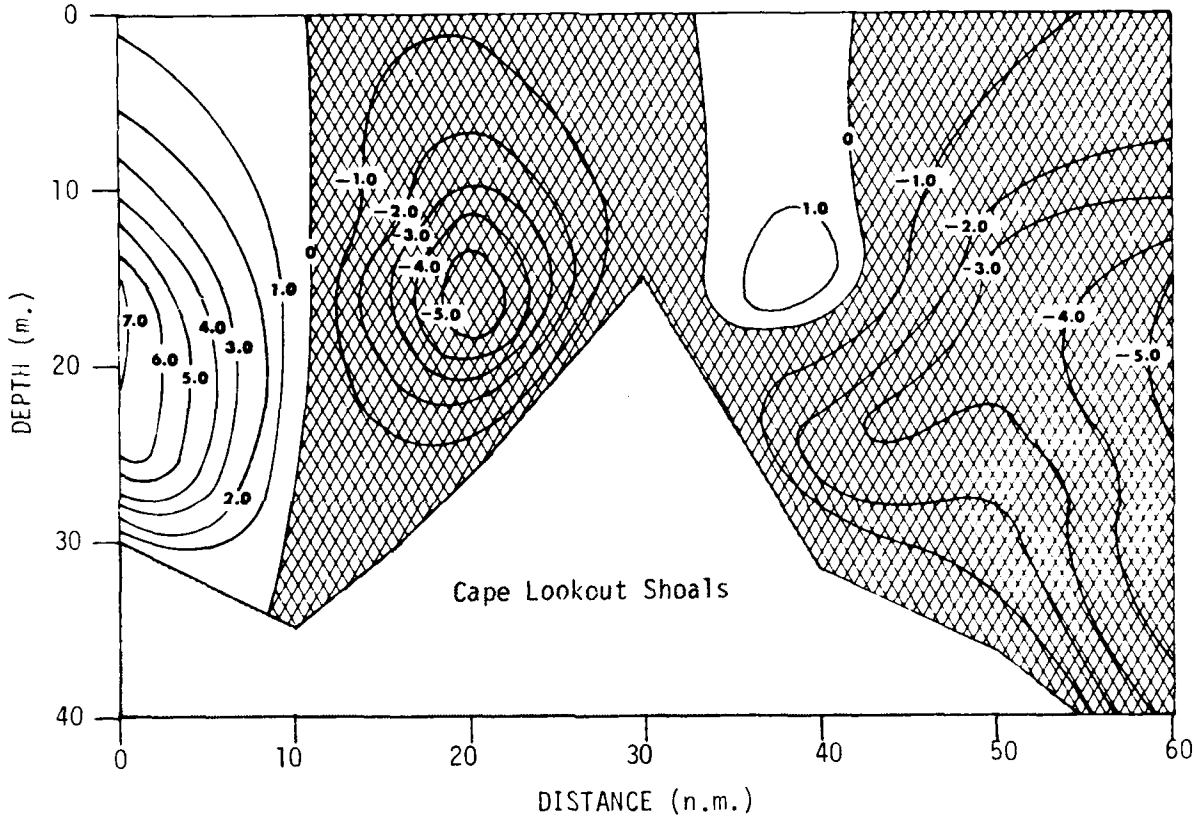

Figure 3.1.2.6 Analysis of geostrophic current (cm s^{-1}). Computations were made relative to the surface. Positive values indicate eastward motion.

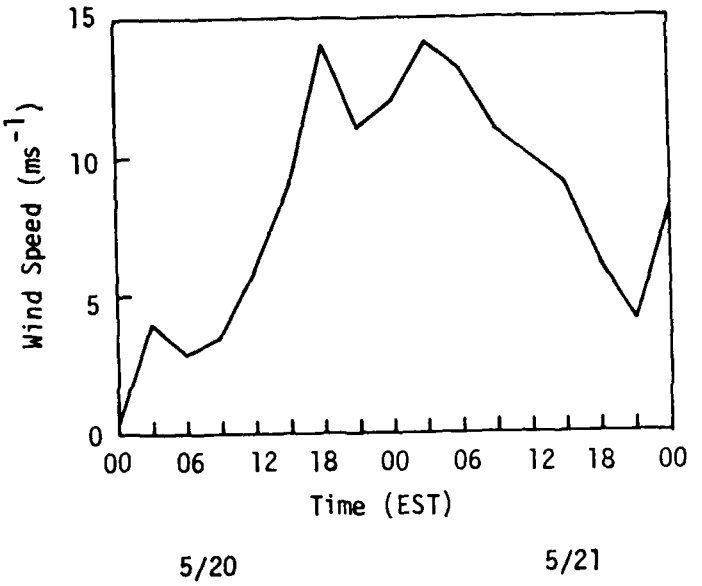

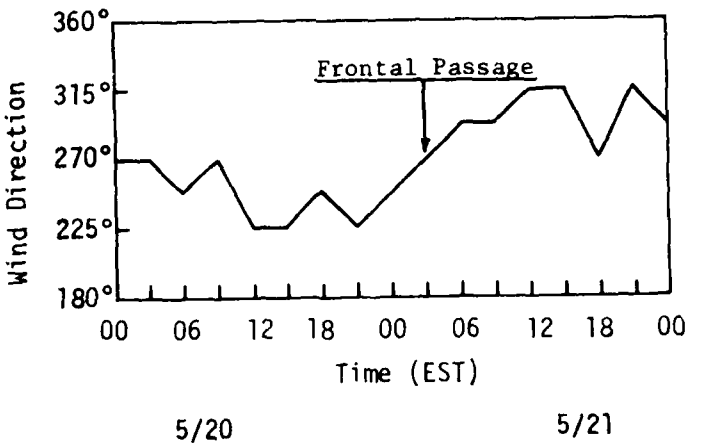

Figure 3.1.3.1 Three-hourly wind data for Diamond Shoals Light Station (35.2°N and 75.3°W).

Figure 3.1.3.2 NOAA-2 VHRR infrared photograph for the southeast coast on 21 May 1973.

Available satellite data gave no indication that this perturbation was present prior to that date. The configuration was reminiscent of the eddies first reported by Rao et al.(1971). South of the eddy in Onslow Bay and east of Cape Romain, a tongue of shelf water
Gulf Stream. On 22 May, two lenses of warm water were present off the coast of the Carolinas (Figure 3.1.3.3 ... also a VHRR infrared image). The first was in Onslow Bay and was the remains of the eddy apparent on 21 May. The second was found in Long Bay; its southern extension was not visible because of cloud interference. Since this lens was not evident in the 21 May data, it is suggested that it was produced as a result of the penetration of the tongue of shelf water east of Cape Romain into the Gulf Stream.

Figure 3.1.3.4 is the sea-surface temperature analysis from the digitized VHRR data. The resolution of the data used in the analysis is 4 km which is a result of averaging. These data were received uncalibrated. In order to calibrate them, and subsequent data, the isotherm interval established by the National Environmental Satellite Service was assumed correct. Under this assumption, it was only necessary to establish the value of one of the isotherms. The surface temperature in the Gulf Stream was determined from the towed thermistor data obtained by the R/V DALLAS HERRING on 23 May. Assuming a quasi steady-state, these data were applied to the digitized VHRR data in the near proximity of the ship's location. A limited estimate of the accuracy attained using this technique is shown in Figure 3.1.3.5 which

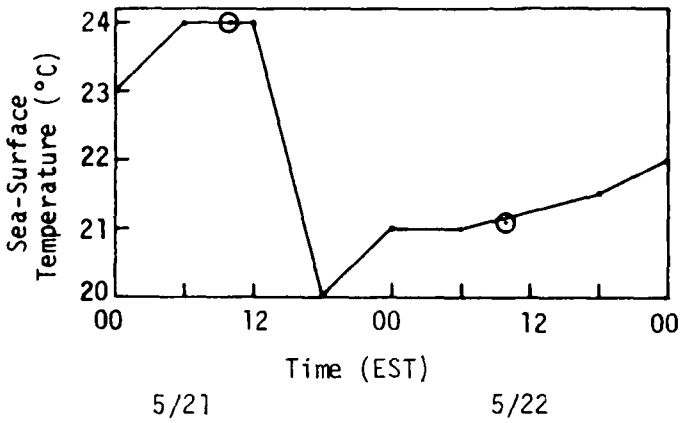

Figure 3.1.3.5 Comparison of sea-surface temperature from Diamond Shoals Light Station (35.2°N and 75.3°W) (solid line) and observed values of sea-surface temperature for NOAA-2 VHRR (data points circled).

Figure 3.1.3.3 NOAA-2 VHR Infrared photograph for the southeast coast on 22 May 1973.

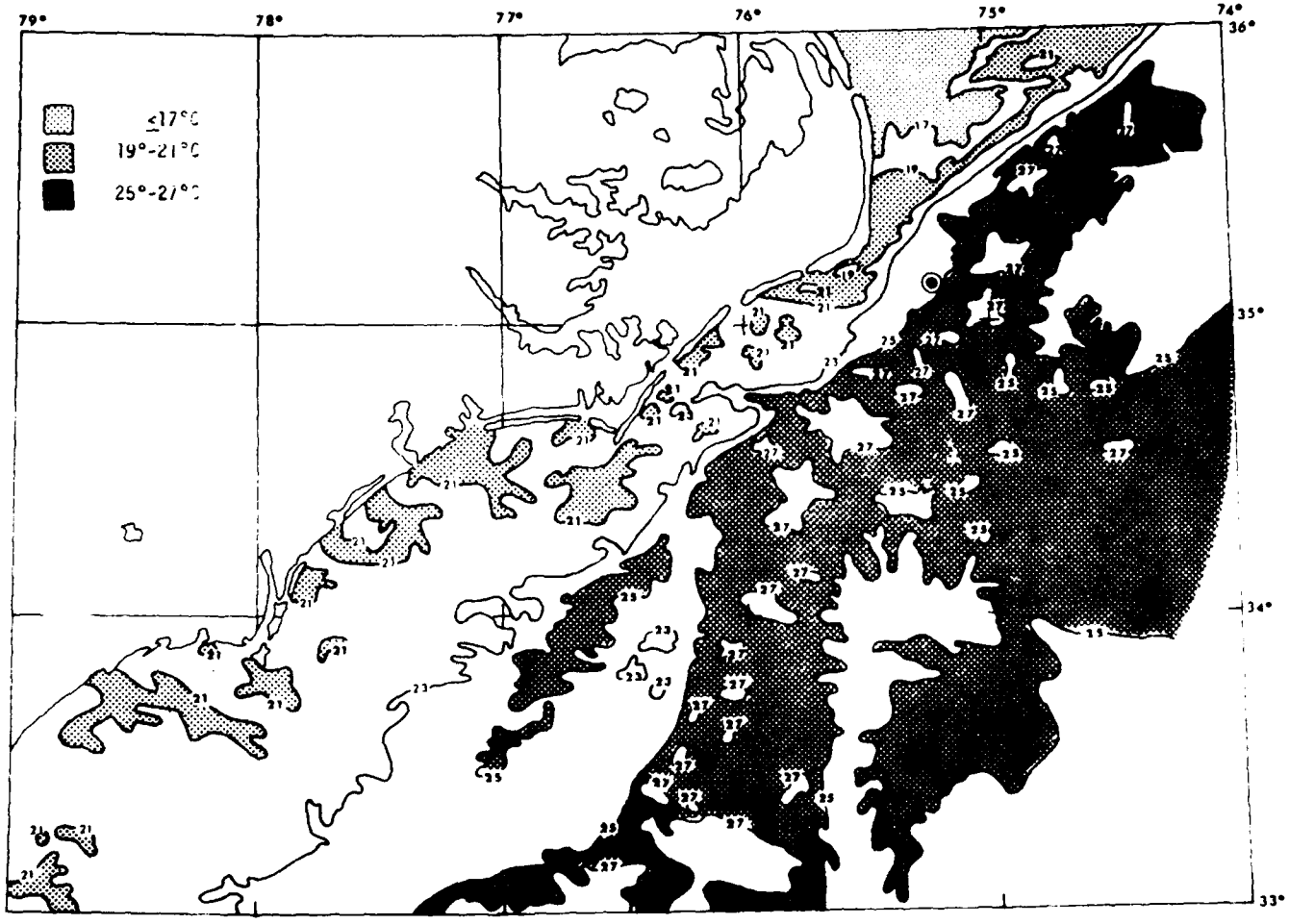

Figure 3.1.3.4 Analysis of sea-surface temperature (°C) using digitized NOAA-2 VHRR infrared data for 21 May 1973. The circled dot represents the position of the Diamond Shoals Light Station.

compares the sea-surface temperatures observed at the Diamond Shoals Light Station (35.2°N, 75.3°W) (see Figure 3.1.3.4) with the satellite observations at the Light Station. Differences are of the order of 0.2°C.

The analysis of the VHRR data for 21 May shows the cut-off, closed lens of warm water (> 25°C) in Onslow Bay whose source was apparently the Gulf Stream. The origin of the cold water (< 23°C) east of the warm lens must be continental shelf.

The sea-surface temperature analysis from the digitized VHRR data for 22 May is given in Figure 3.1.3.6. There was considerable cloud interference on this day to the south, to the east, and in Onslow Bay, but the main features are evident. The lens of warm water (> 25°C) in Onslow Bay, found on 21 May, has decreased in area and the center of the lens is located to the north of its position on 21 May (34.25°N, 76.5°W). This lens decreased to less than one-half its size in twenty-four hours. The second lens (also > 25°C) is east of Cape Fear (33.75°N, 76.5°W).

The R/V DALLAS HERRING collected data along two transects on 22-23 May. These transects, shown in Figure 3.1.3.7, were in the lens formed between 21 and 22 May. Figure 3.1.3.8 yields the temperature analysis along the first transect and shows the warm lens located over the shelf break (between Stations 2 and 3). The lens is considerably narrower (16 km) than depicted in the satellite data (48 km). Figure 3.1.3.9 yields an analysis for the first 20-m depth along the first transect. For this analysis, the surface thermistor data were combined with the subsurface data which were chosen at 2.5 m intervals. From the analysis, it would appear that the warm lens is not much more than 15-m deep.

The salinity data (Figure 3.1.3.10) for Station 4 in the Gulf Stream indicated that at this time and in this region, the first 60-m depth of the Gulf Stream had constant salinity with a value of 36.6 $^{\circ}/_{\circ\circ}$; below 60 m, the salinity increased. At Station 3 in the transition zone between the warm lens and the shelf water, the salinity was generally lower in value than at Station 4. The lowest value (36.2 $^{\circ}/_{\circ\circ}$) was found at the 20-m level; and below that level, the salinity increased, reaching a value consistent with the upper levels of the Gulf Stream at the 60-m level. The variability in the salinity profile for the first 60 m at Station 3, suggests the possibility that the shelf water separating the warm lens from the Gulf Stream

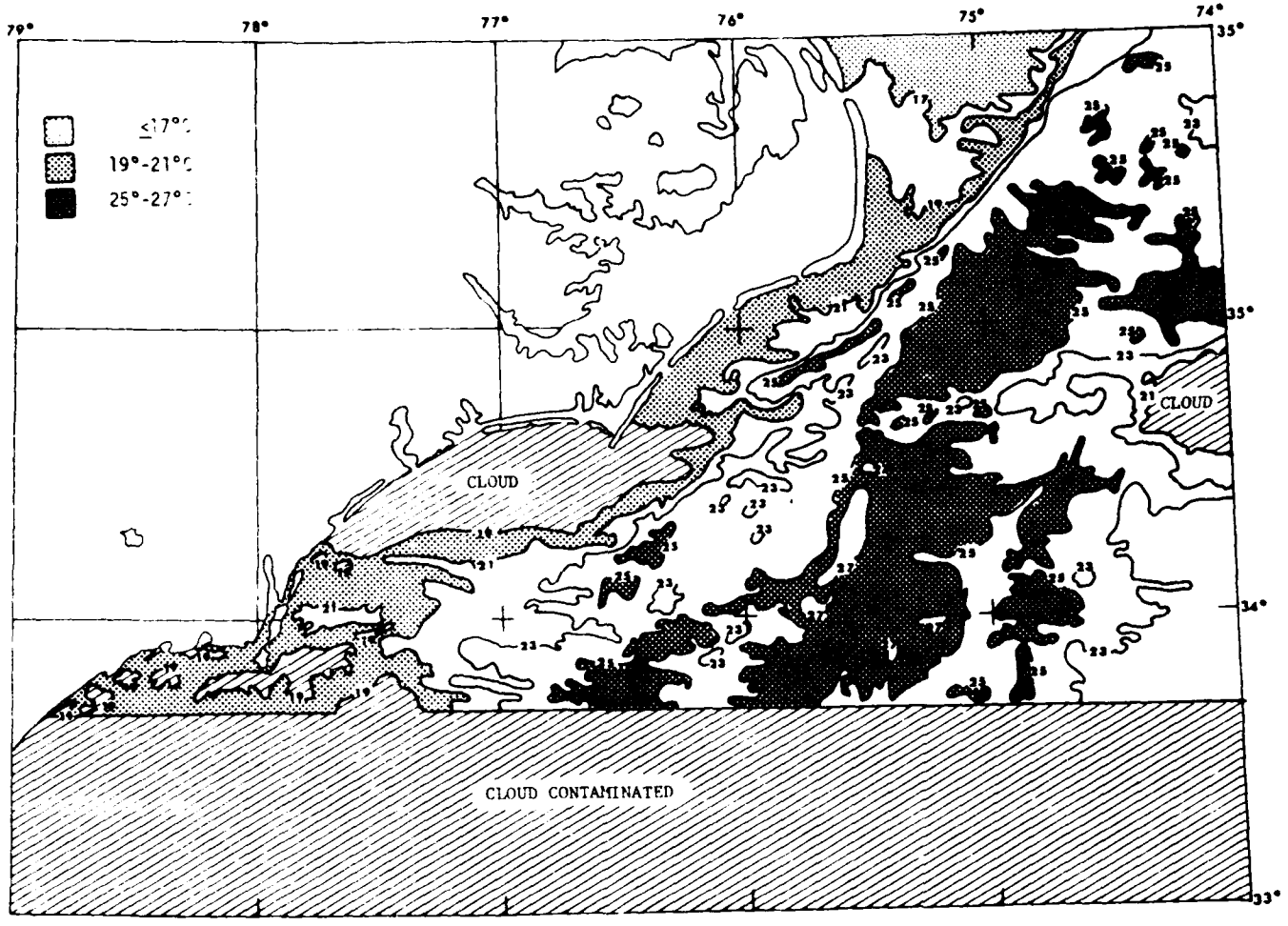

Figure 3.1.3.6 Analysis of sea-surface temperature (°C) using digitized NOAA-2 VHRR infrared data for 22 May 1973.

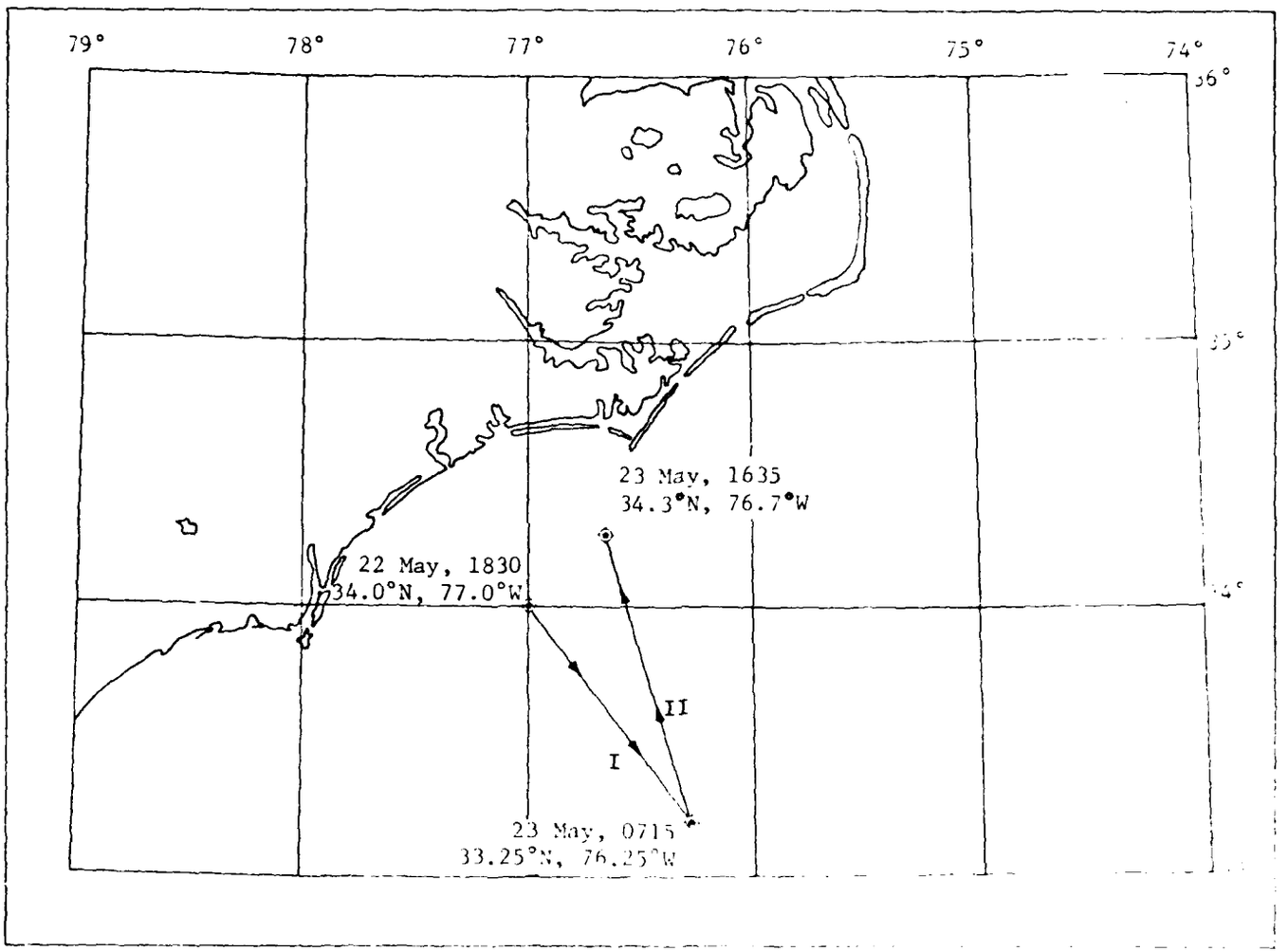

Figure 3.1.3.7 Track of R/V DALLAS HERRING between 22 May-23 May 1973.

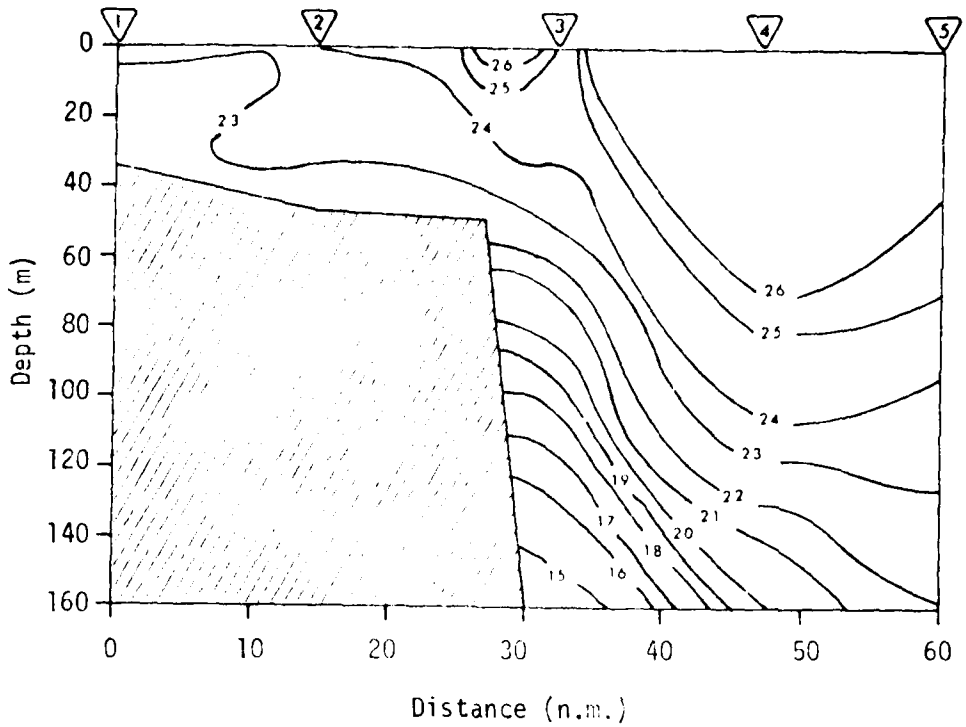

Figure 3.1.3.8 Vertical temperature (°C) cross-section from data collected by R/V DALLAS HERRING along the track marked I. Station numbers are given at the top of the figure.

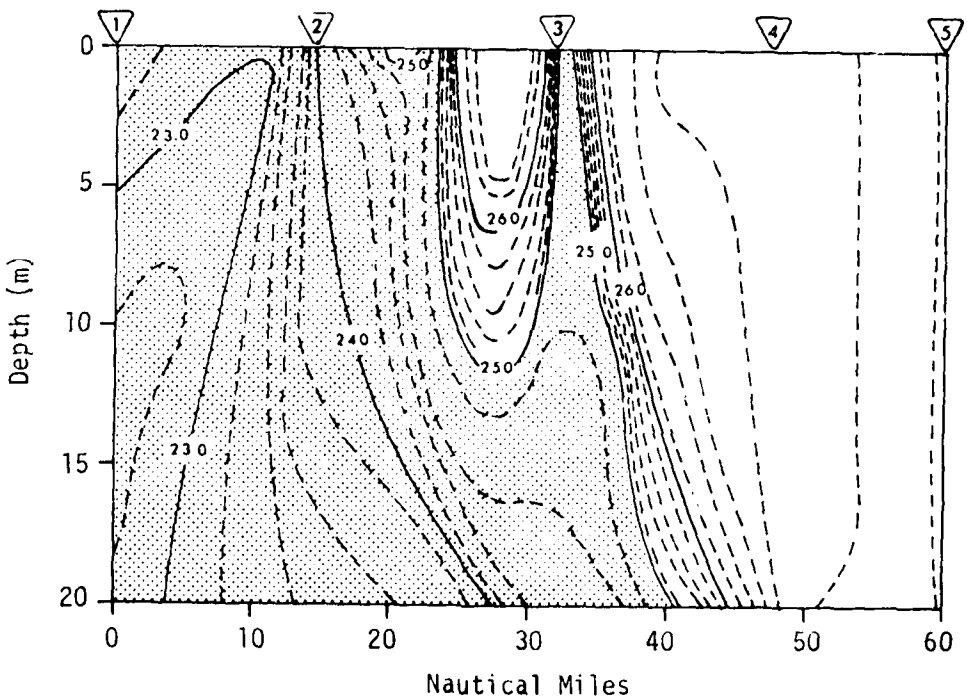

Figure 3.1.3.9 High resolution temperature (°C) analysis of the first 20 meters along the track marked I in Figure 15. Station numbers are given at the top of the figure.

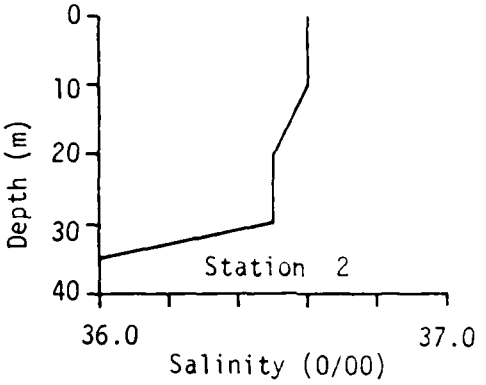

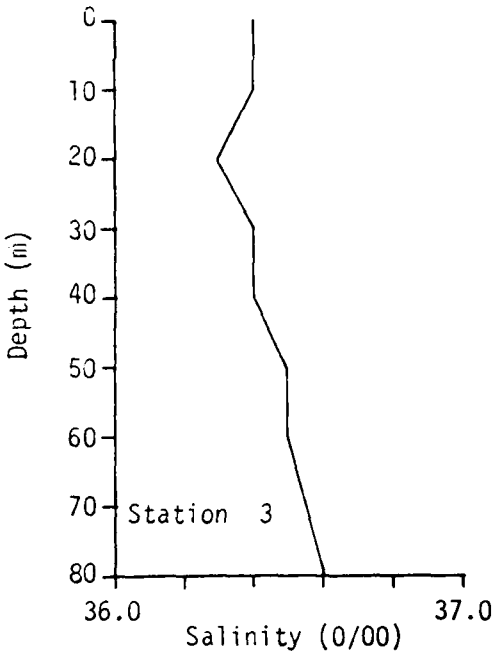

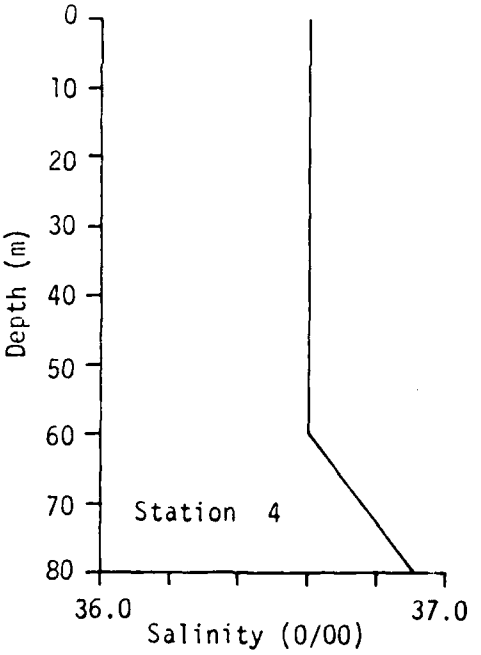

Figure 3.1.3.10 Salinity profiles for Stations 2, 3 and 4.

may have been much deeper than the temperature data in Figure 3.1.3.9 indicated. In the first 10 m at Station 2, the salinity has values consistent with those in the upper levels of the Gulf Stream (36.6 °/₀₀) suggesting that the warm lens, whose source is the Gulf Stream, may have extended to Station 2 at one time.

According to the temperature analysis for the second transect (Figure 3.1.3.11), the warm lens also over the shelf break in this case, was 30-km wide which compares somewhat favorably with the width of the lens in this region determined from the 22 May satellite data analysis (40 km). The vertical extent of the lens, which can be more easily resolved using Figure 3.1.3.12 (same data format used for this analyses as for that in Figure 3.1.3.9) appears to be about 25 meters. The salinity data (Figure 3.1.3.13) for Station 4, which yields the local characteristics of the Gulf Stream, indicate the same general characteristics as Station 4; i.e., the first 60 m has constant salinity with a value of 36.6 °/₀₀ and the salinity increased below the 60 m level. At Station 7 (i.e., in the approximate center of the warm lens), the salinity is constant down to 30 m with a value of 36.6 °/₀₀, consistent with that found in the upper region of the Gulf Stream. Below 30 m, the salinity decreases; this characteristic must be attributed to the existence of shelf water below the warm lens. These data suggests that the depth of the warm lens is approximately 30 m.

3.1.4 Summary and Conclusions

Both case studies demonstrate an exchange of shelf water with Gulf Stream water south of Cape Hatteras. However, the exchanges seem to be somewhat one-sided in that a lens of Gulf Stream water becomes isolated on the shelf, but there is no apparent isolation of shelf water in the Gulf Stream. The approximate life cycle of the entire event from the production to the eventual absorption of the lens of Gulf Stream water on the shelf appeared, from the data available, to be not much more than 72 hours.

Many mechanisms have been proposed for the production of eddies on the western boundary of the Gulf Stream. Most prominent of these is baroclinic instability combined with bottom topography. However, this

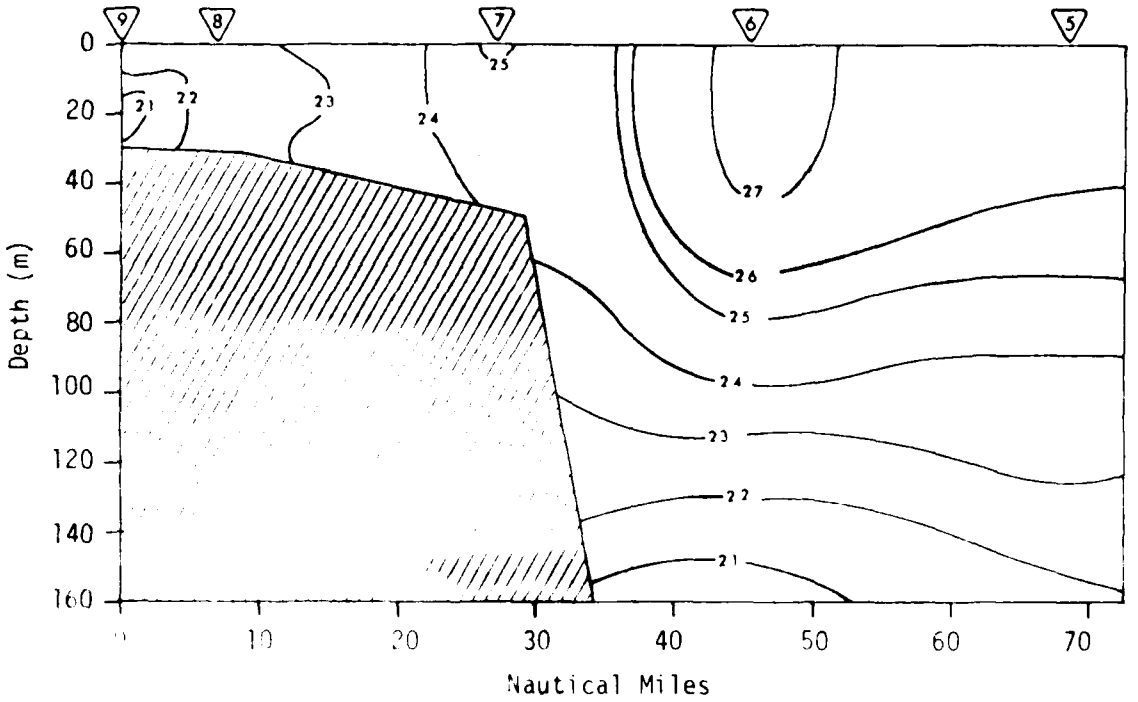

Figure 3.1.3.11 Vertical temperature (°C) cross-section from data collected by R/V DALLAS HERRING along the track marked 11. Station numbers are given at the top of the figure.

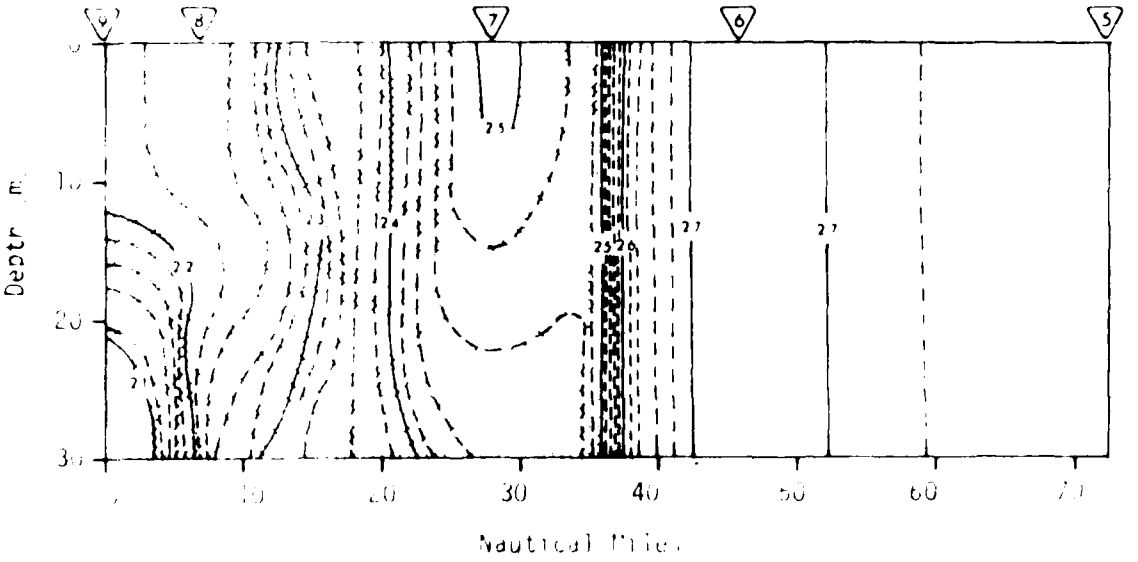

Figure 3.1.3.12 High resolution temperature (°C) analysis of the first 20 meters along the track marked 11. Station numbers are given at the top of the figure.

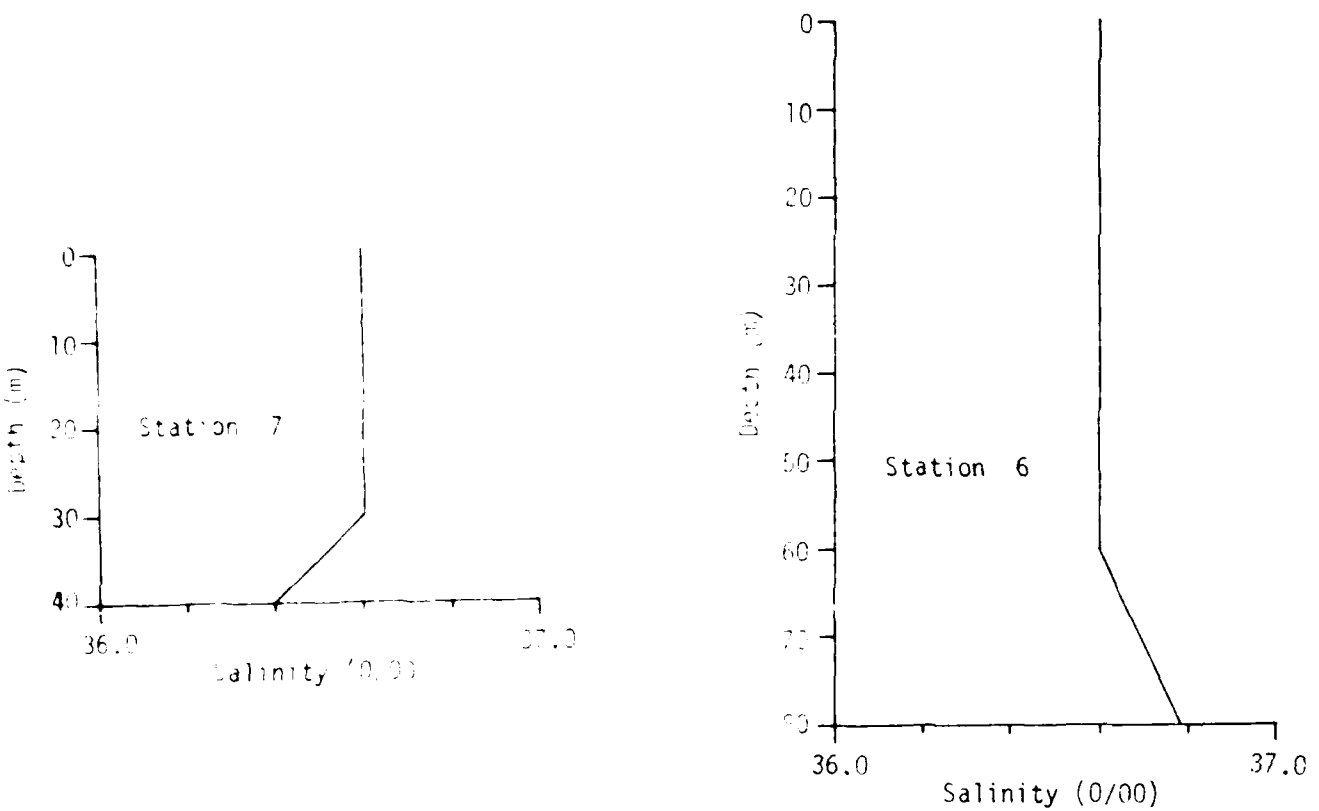

Figure 3.1.3.13 Salinity profiles for Stations 6 and 7.

mechanism leads to eddies having a life cycle much longer than that indicated by these data. For instance, the eddies reported by Rao et al. (1971) were evident for at least 14 days (personal communication). This suggests that there is a fundamental difference between the eddies observed in this case and those produced baroclinically.

The following hypothesis for the mechanics of the exchange process evolved from the data presented (see Figure 3.1.4.1). A tongue of cold shelf water penetrates into the Gulf Stream (Frame #1) similar to that shown on 21 May, VHRR data. The northward flow in the Gulf Stream in this region provides a northward impetus to the tongue, and the momentum flux associated with horizontal shear in the Gulf Stream current would transport the tongue of shelf water back to the shelf (Frame #2). The end result is the isolation of a lens of Gulf Stream water (Frame #3). The depth of the lens is probably related to the depth of the shelf water, approximately 30 to 60 m. After the lens is cut off, the influence of the Gulf Stream current and shear stress at the western boundary of the Gulf Stream would stretch the axis of the lens parallel to that boundary and compress the axis of the lens perpendicular to that boundary (Frames #4 and #5), thus, narrowing the width of the lens as demonstrated in the satellite and ship data for 22 and 23 May.

One of the most important driving forces for the production of currents on the shelf is the wind. In each of the case studies presented, there were sustained periods of strong winds which could have created strong currents. South of Cape Hatteras, the north northeast to south southwest orientation of the shelf would influence markedly the direction of motion of the wind-driven currents on the shelf; but, it would appear from the 5-8 May case study that shoaling also affect the direction of motion. Shoals exist off Cape Fear (Frying Pan Shoals), Cape Lookout (Cape Lookout Shoals), and Cape Hatteras (Diamond Shoals), and to a lesser extent, off Cape Romain. These shoals could direct mass flow on the shelf eastward, leading to the penetration of a tongue of shelf water into the Gulf Stream and the sequence of events described above (Rao et al., 1971).

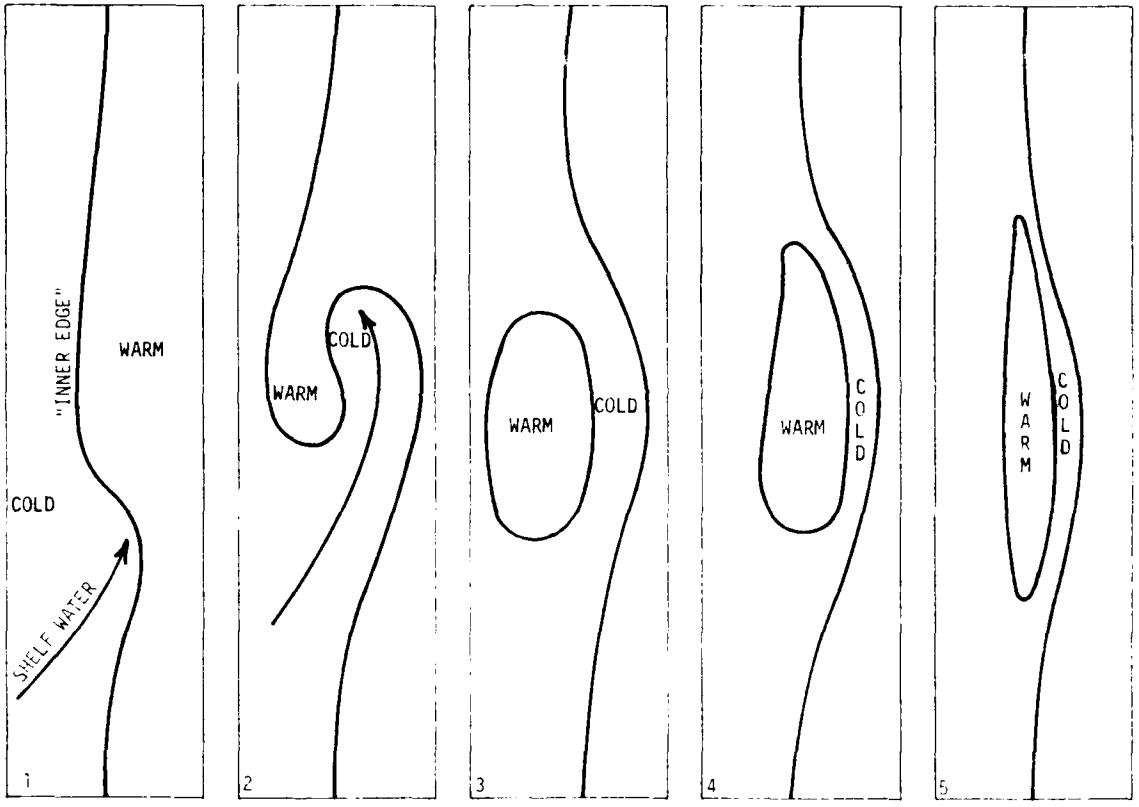

Figure 3.1.4.1 Schematic of the development of an isolated lens of the Gulf Stream water on the shelf.

3.2 A Study of a Cyclonic Cold Eddy on the Eastern Side of the Gulf Stream

3.2.1 General

Recently, there has been some interesting observations of cold eddies near the eastern boundary of the Gulf Stream via infrared imagery from satellites (Richardson, Strong and Knauss, 1973; and Stumpf, Strong and Pritchard, 1973). These eddies, sometimes called Gulf Stream rings (Parker, 1971) consisted of a cold central core surrounded by a ring of warm, presumably Gulf Stream water. It has been suggested that the central core is less saline slope water. The limited observed data on the genesis of these eddies have suggested that they form between 60°W and 70°W longitude on the "north wall" of the Gulf Stream through instability which causes a portion of a Gulf Stream meander to "break away" from the north wall and so producing a separate entity from the Gulf Stream current south of that current.

Though there is no concrete evidence, it is believed that the circulation within the eddy is cyclonic. The eddy system appears to move with a speed of about one mile per day (Richardson et al., 1973). The lifetime of these eddies is unknown. However, the results of an investigation using observations made over a four-month period indicate that the eddies may have a projected life anywhere from three to five years (Barrett, 1971). Since many of these eddies are absorbed by the Gulf Stream (Parker, 1971 and Richardson et al., 1973), the above estimates of the eddy's lifetime, which is based solely on the interval of energy dissipation, are upper limits.

The following describes the results of a study combining NOAA-2 and NOAA-3 infrared imagery with conventional in-situ data to glean further information concerning one of these cold eddies. Based on the available data, the eddy in question apparently had its genesis near the end of August 1973. It was first observed on 31 August 1973 (see Figure 3.2.1.1) at about 36°N and 68°W. The evidence indicated that it moved almost directly westward when on 28 November 1973, it was located at about 36°N and 72°W. Afterwards, it moved southwestward and was located at about 33°N and 74°W on 1 April 1974. These data suggested an average speed of the cold eddy system of about 5.6 km/day.

During the spring of 1974, periods of clear skies enabled the radiometers on NOAA-2 and NOAA-3 to obtain some rather remarkable infrared

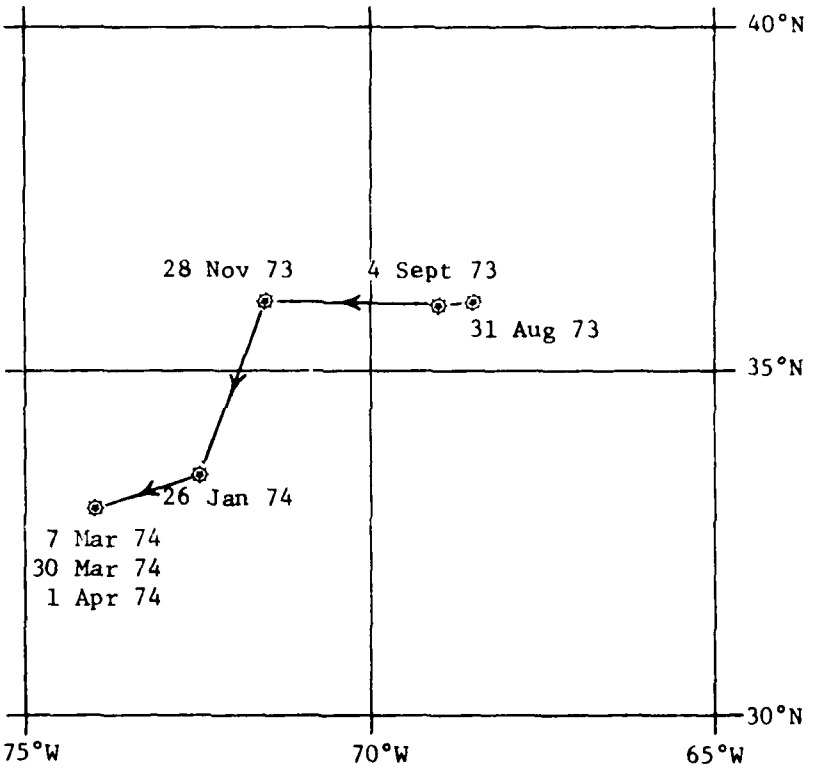

Figure 3.2.1.1 Plot of the location of the cold eddy between 31 August 1973 and 1 April 1974.

infrared images off the southeast coast of the United States. The VHRR image for 7 March 1974 (Figure 3.2.1.2) shows that a number of meanders existed along the western and northern boundaries of the Gulf Stream. On the north wall of the Gulf Stream, the rather pronounced meander (upper righthand side of the figure) is the type of perturbation required to produce cold eddies. The cold eddy of interest is located at 33 N and 74 W, just east of the Gulf Stream (dark region in photograph). The warm ring around the eddy is clearly visible.

The cold eddy was visible again on 1 April 1974 (Figure 3.2.1.3). It appeared that in the 25-day period between this observation and the previous 7 March observation, the cold eddy did not change location. The warm ring around the eddy is still evident, but the surface area of the eddy appears to have reduced in size.

On 25 March 1974, the R/V ADVANCE II was sent into the region of the cold eddy to collect surface and subsurface salinity and temperature data along three separate transects. The transects were determined from the NOAA-2 IR image for 7 March. The position of the intial end points of each transect are given in Table 3.2.1.1. The transects are also shown in Figure 3.2.2.3.

Table 3.2.1.1 The position of the initial station and the last station for each transect made during the period 27 to 29 March 1974. Each transect was as near to a straight line as possible.

Transect	Position of Initial Station	Position of Last Station
I	33.00°N Latitude 75.00°W Longitude	33.00°N Latitude 72.00°W Longitude
II	32.42°N Latitude 72.00°W Longitude	32.42°N Latitude 75.00°W Longitude
III	32.42°N Latitude 75.00°W Longitude	33.00°N Latitude 73.80°W Longitude

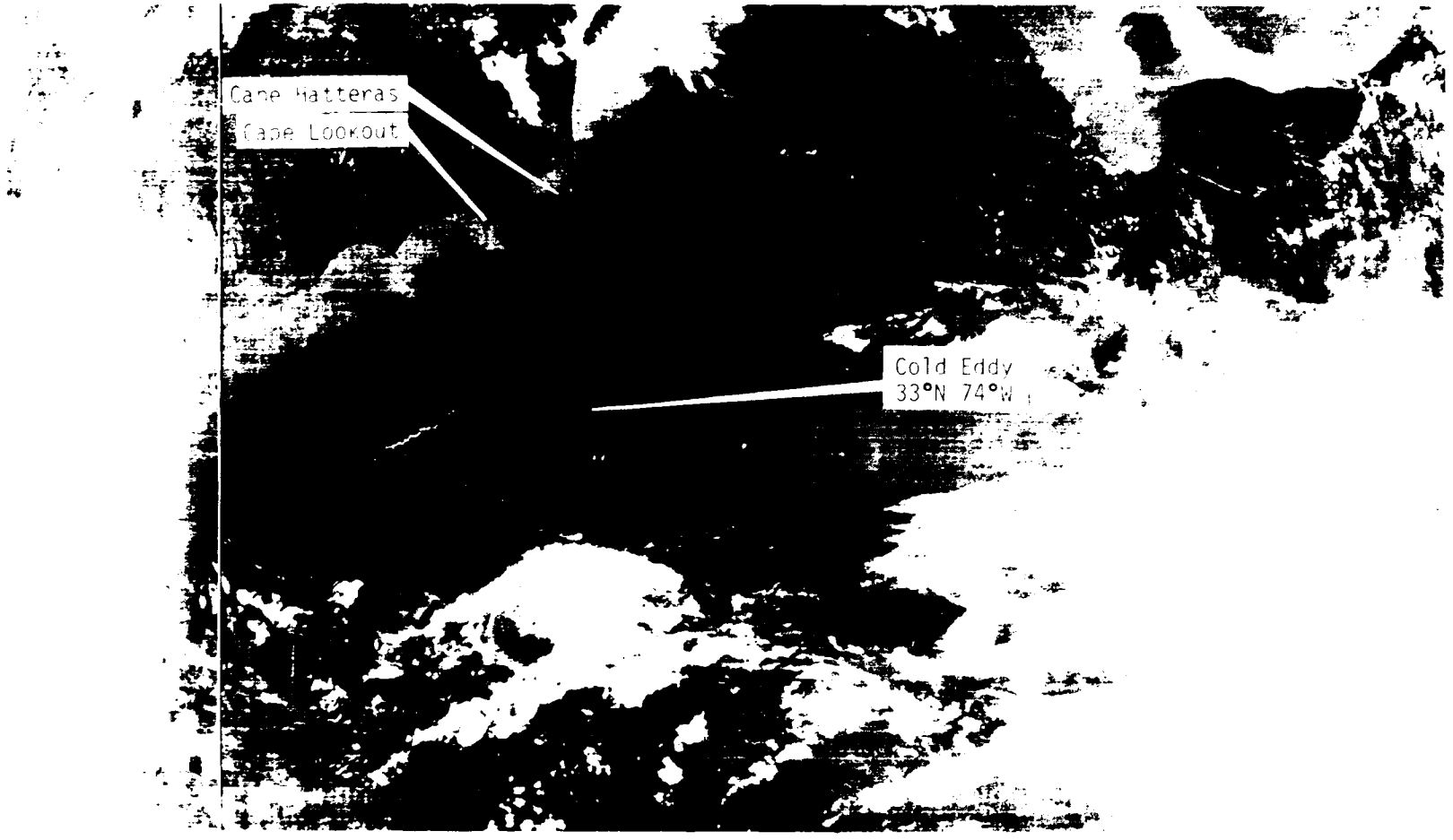

Figure 3.2.1.2 NOAA-2 VHRR infrared image for the southeast coast on 7 March 1974.

Figure 3.2.1.3 NOAA-3 VHRR infrared image for the southeast coast on 1 April 1974.

3.2.2 Horizontal Temperature Structure of the Cold Eddy

The 7 March and 1 April satellite data used for analysis were received uncalibrated. In order to calibrate them, the isotherm interval established by the National Environmental Satellite Service (1°C) was assumed correct. The value of one of the isotherms was established by using the surface temperature data obtained in the central core of the cold eddy by the R/V ADVANCE II. Figure 3.2.2.1 gives a comparison of the sea-surface temperatures obtianed by the R/V ADVANCE II along the three transects and that observed by NOAA-2 on 7 March and by NOAA-3 on 1 April along the same transects. The ADVANCE II data in the cold eddy along Transect I were used to calibrate the satellite data, which accounts for the excellent agreement between the surface truth and 1 April satellite data in that region. If the position of the cold eddy on 7 March is aligned with that given by the surface data and by 1 April satellite data, it, too, would compare well with surface truth data. There were, however, discrepancies between the satellite data and surface truth data east of the cold eddy along Transect I and all along Transects II and III after the positions of the eddy were aligned. On the average, the surface truth temperature was about 1.0°C higher than the satellite sea-surface temperature in these cases. After alignment of the cold eddy, however, there was good agreement between the satellite data for 7 March and 1 April. Atmospheric attenuation of any kind cannot account for the 1.0°C discrepancy between surface truth and satellite data, since the technique used to calibrate the satellite data would eliminate this source of error. The difference may be a result of the fact that the satellite radiometers measure the "skin temperature" of the sea-surface (i.e., first 20 μm) which has generally a lower temperature than the water in the first few centimeters measured by the towed thermistor [Ewing and McAlister, (1960)].

Figure 3.2.2.2 gives the sea-surface temperature analysis off the North Carolina coast on 7 March 1974. The cold eddy is located, as indicated earlier, at about 33°N, 74°W. The surface temperature in the central regions of the eddy lies between 18°C and 19°C. A region of warm water (> 20°C) encircles the cold eddy. The eddy has an elliptical shape.

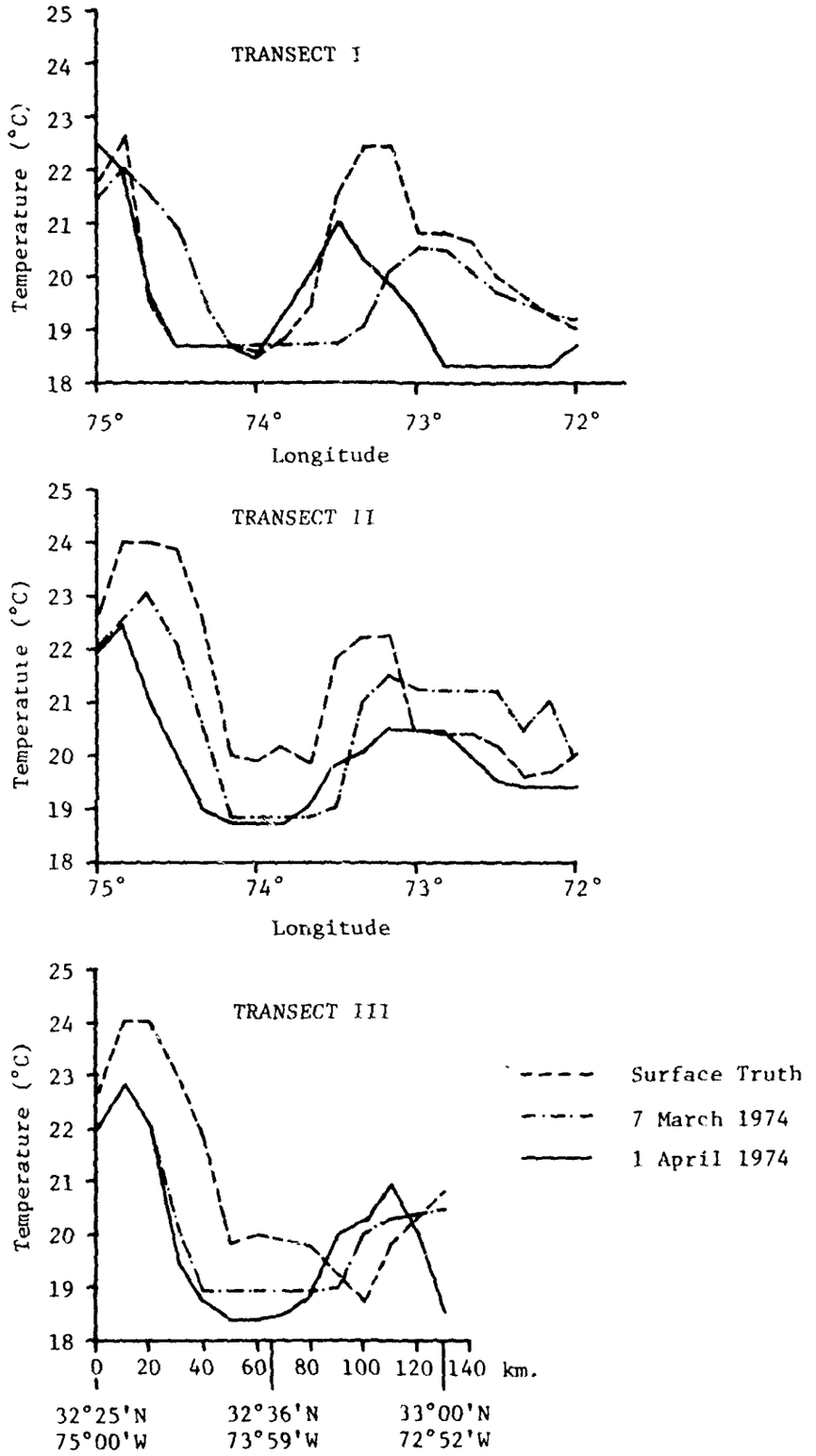

Figure 3.2.2.1 Comparison between the sea-surface temperature (°C) data collected by the R/V ADVANCE II for the period 27-29 March, 1974 along all three transects and the 7 March and 1 April VHRR data along the same transects.

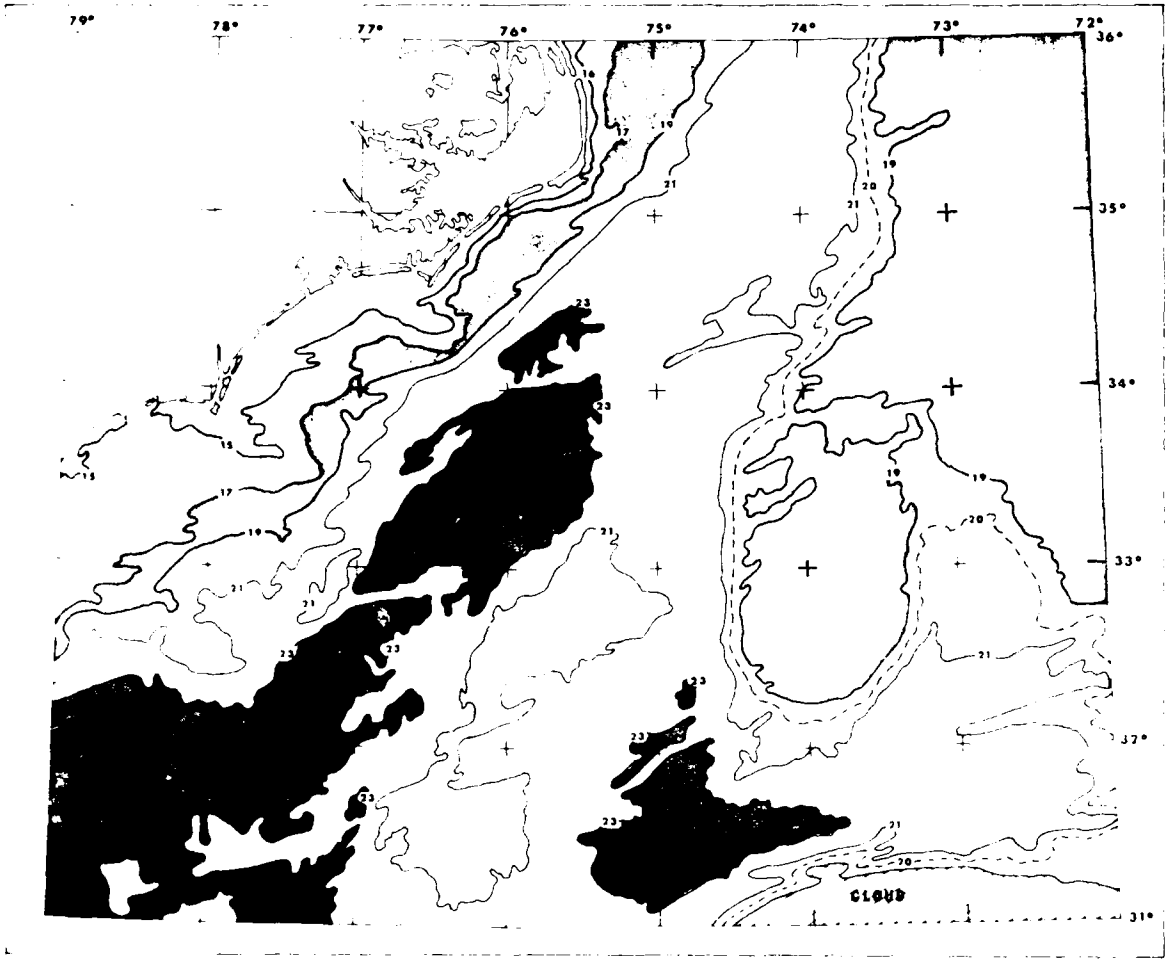

Figure 3.2.2.2 Sea-surface temperature analysis (°C) using digitized NOAA-2 VHRR data for 7 March 1974.

Using the 19°C isotherm to define the eddy, the major axis is oriented north-south and is approximately 180-km long. The minor axis is 120-km long.

The sea-surface temperature distribution for 1 April 1974 (Figure 3.2.2.3) shows the cold eddy to be located in approximately the same position as on 7 March analysis (33°N, 75°W). This figure also contains a graphical diagram of the transects. The eddy still appeared to be elliptical, but the overall dimensions had decreased. The major axis was oriented northwest-southeast suggesting a cyclonic rotation. Again, using the 19°C isotherm, the length of the major axis was approximately 120 km, and that of the minor axis was 100 km. The warm ring (water temperature in excess of 20.5°C) is very distinct.

The orientation of the isotherms in the vicinity of the cold eddy for the 7 March and 1 April VHRR sea-surface temperature analysis, suggest that the circulation of the cold eddy is entraining Gulf Stream water reinforcing the warm ring around the eddy; i.e., the warmest water in the warm ring is on the Gulf Stream side of the eddy where there is no marked distinction between the Gulf Stream and warm ring, suggesting a coalescence. They further suggest that the circulation of the eddy is cyclonic since there is a tongue of warm water wrapping around the eddy in a cyclonic sense originating from the region of coalescence.

The surface temperature in the central core of the cold eddy on 1 April was about 0.5°C less than that on 7 March. The existence of this region on 1 April is based on the presence of a closed isotherm south of the region where the satellite data were calibrated. No such isotherm existed in the 7 March data. The calibration data suggested that the value of that isotherm was 18.5°C. This apparent cooling is suspect, since it is believed that the eddy is dissipating which should cause a gradual warming. One explanation for the apparent cooling is sensor degradation. The data collected on 7 March was accomplished by the sensors on NOAA-2 which was on its 6300 orbit; but for 1 April, NOAA-3 sensors were used which was only on its 1800 orbit. The apparent cooling may have been a result of reduce sensitivity due to degradation of the NOAA-2 sensors.

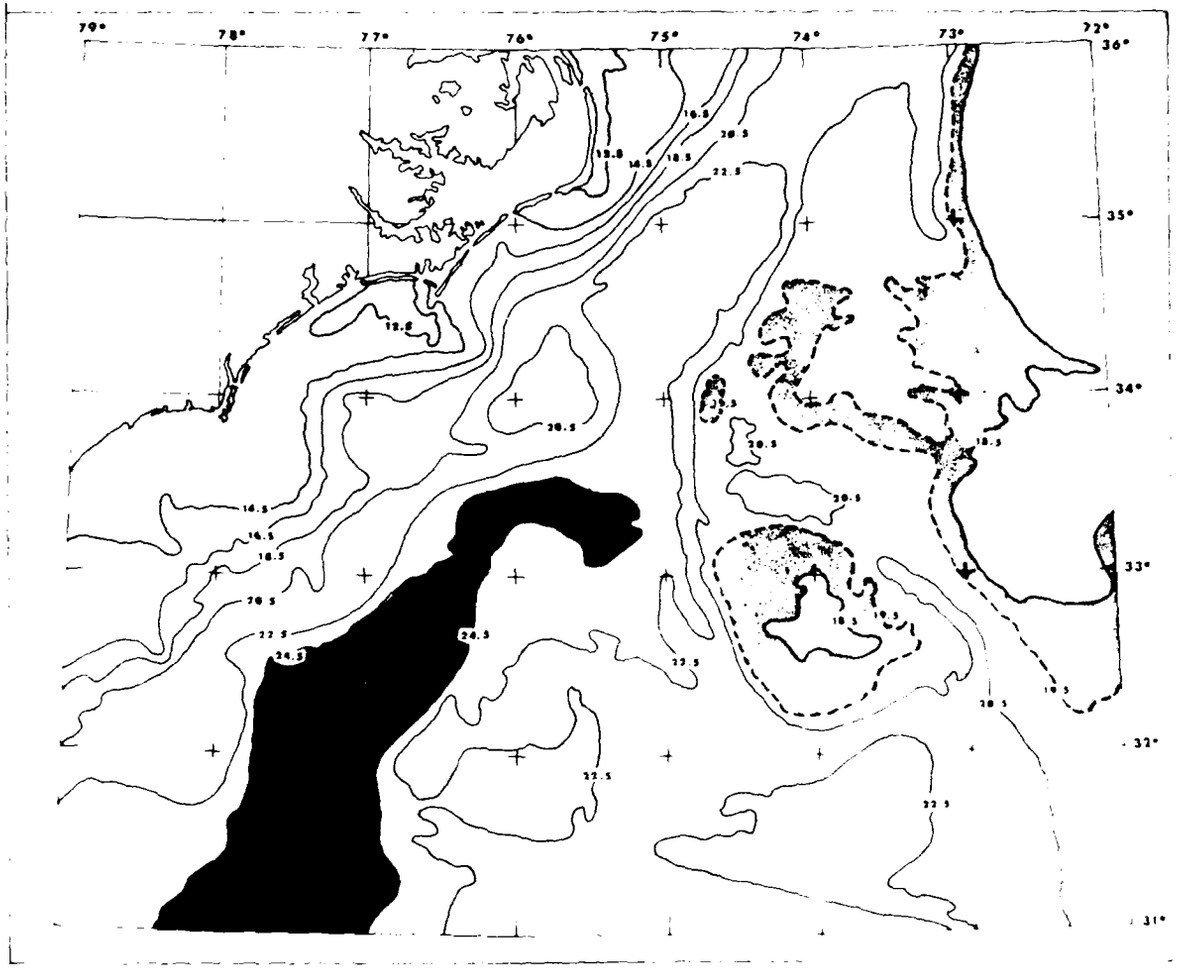

Figure 3.2.2.3 Sea-surface temperature analysis (°C) using digitized NOAA-3 VHRR data for 1 April 1974. Transects I, II and III are also indicated.

The subsurface temperature data obtained by the R/V ADVANCE II were integrated to produce an analysis of the horizontal temperature distribution at the 300-m and 500-m level in the region 32°N to 33°N and 75°W and 73°W. The integration period was 27-29 March 1974. The data from Transects I, II and III allowed analysis of only the southern half of the eddy.

The analysis of the 300-m data (Figure 3.2.2.4) indicates that the subsurface center of the eddy was near 33°N, 74.2°W. The lowest temperature at the 300-m level is 14.2°C. The eddy is oriented northwest-southeast similar to the orientation indicated in the surface analysis of 1 April 1974. Using the 17°C isotherm, the minor axis appears to be about 100-km long, again similar to that found on the surface on 1 April. If the eddy were bisected by the 33°N latitude line, then the major axis would be about 120 km, also identical to that found at the surface.

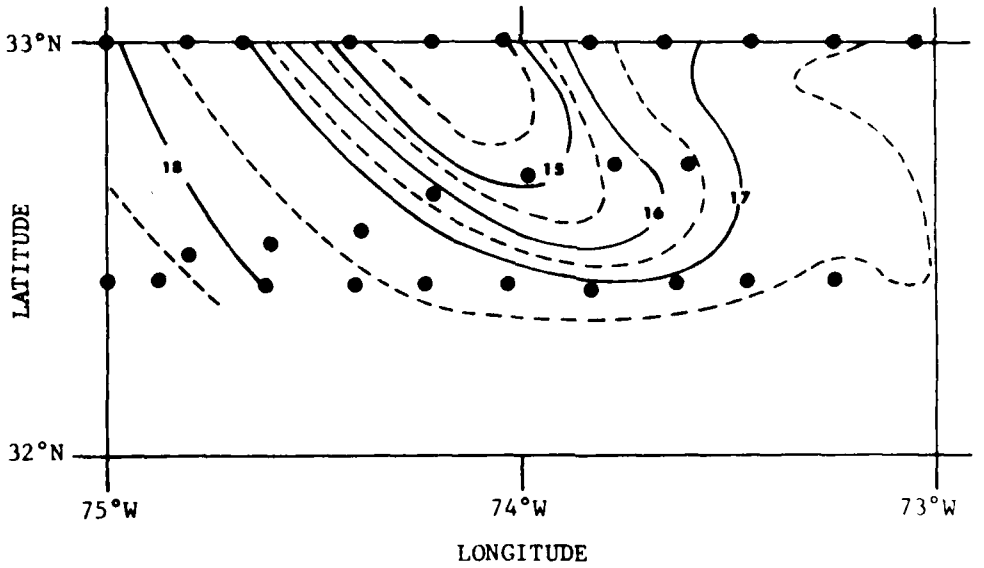

Figure 3.2.2.4 The 300-m temperature analysis (°C) integrating data along Transects I, II and III and for the period 27-29 March 1974. The dots represent location of stations.

The 500-m temperature analysis (Figure 3.2.2.5) indicates that the center of the cold eddy was near 33°N and 74.1°W suggesting a slight

vertical tilt [illegible] the axis of the [illegible] eddy with the 500 m [illegible] to the west of the 500 m center. The lowest temperature at the [illegible] was 11.4°C. The orientation of the eddy was [illegible] rather than northwest southeast as in the upper level [illegible] isotherm, the lengths [illegible] the major and minor axes were about the [illegible] as for the upper levels.

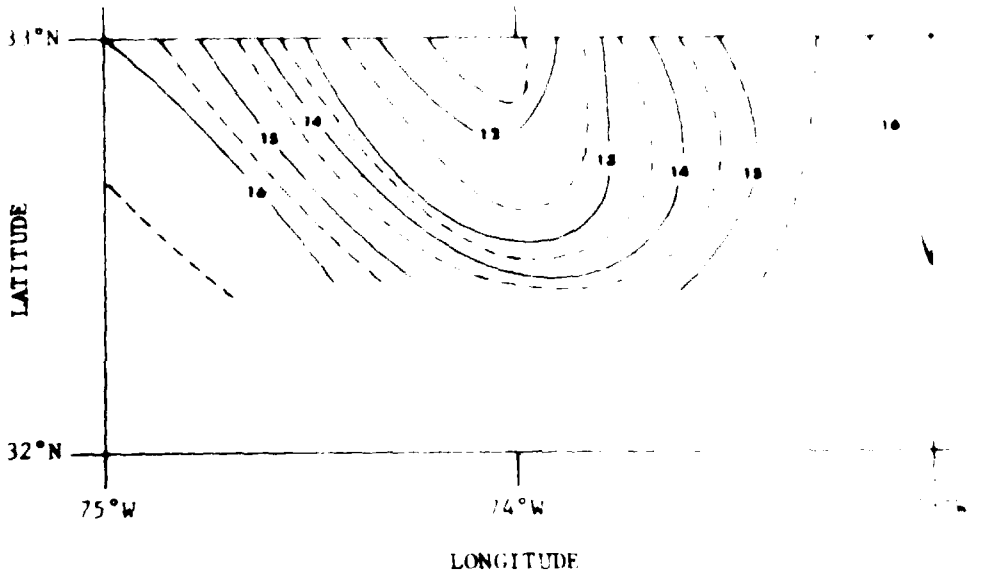

Figure 3.2.3.5 The 500-m temperature analysis [illegible] along Transects I, II and III and for the [illegible] 27-29 March 1974.

3.2.3 The Vertical Structure of the Cold Eddy

The temperature distribution along the first transect is given in Figure 3.2.3.1. The integration period is 0230-0500 EST, 27 March 1974. The cold eddy is made up of two parts: a region below 200 m where the water changes temperature rapidly in the vertical which will be called a cold dome, and a region above 200 m where the water has uniform temperature of about 18.7°C but which is colder than the water east or west of it. The coldest water (11.4°C) is located at lowest level monitored (500 m). The westward tilt of the axis of the cold water is

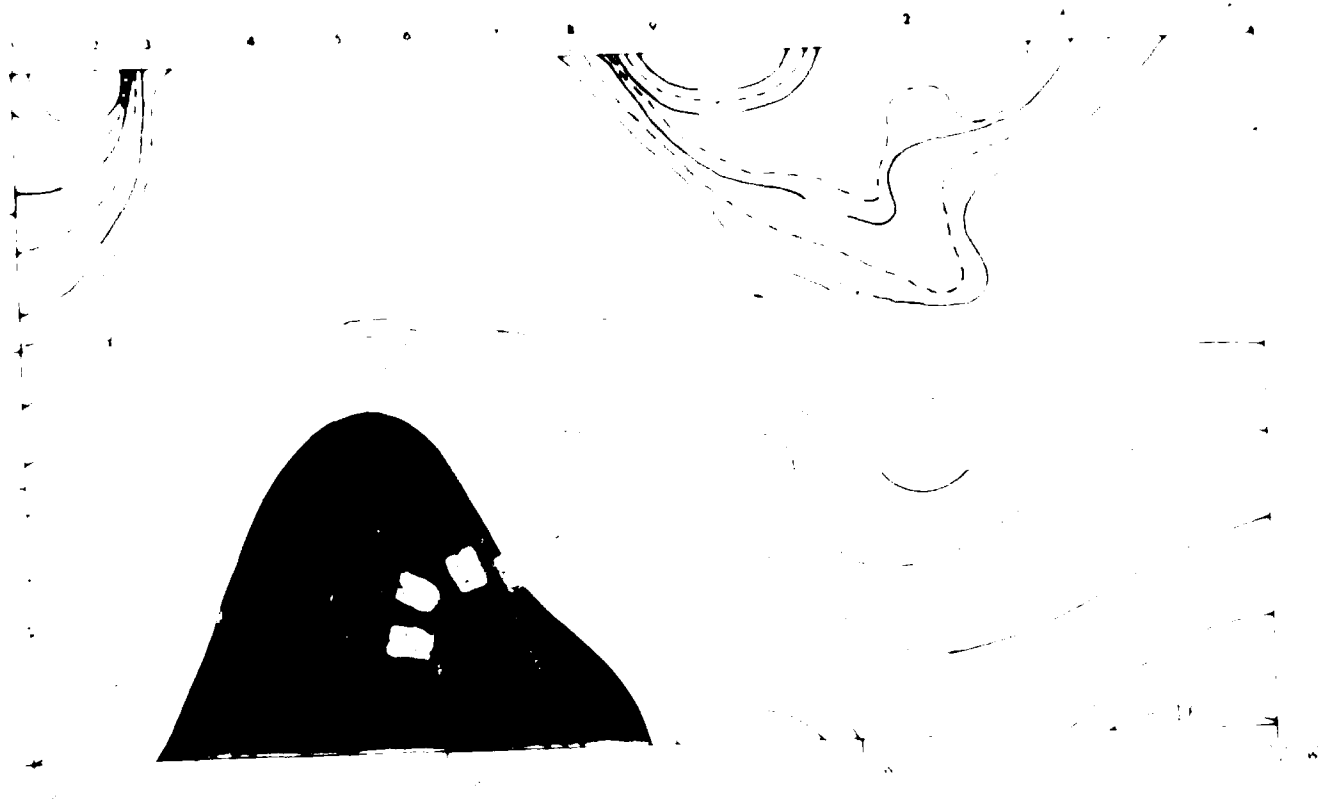

evident in this analysis also, but appears to be restricted to the depths 300 m or greater.

Both the east and west sides of the warm ring are evident; and the maximum temperatures are found at the surface and are equivalent on both sides of the warm ring (22.4°C). The satellite data (Figure 3.2.2.2) suggests that the western side of the warm ring at 33°N should have a higher temperature (i.e., the NOAA-3 data has a maximum temperature of greater than 22.5°C on the western side and has a maximum temperature of approximately 21.0°C on the eastern side along the 33°N latitude line). Differences may be due to effects occurring during the intervening five days between observations. Using the 19°C isotherm, the warm ring extends down to about the 250-m level on both sides of the eddy. The eastern side of the warm ring is about 130 km wide which is larger than the minor axis of the cold eddy. The dimensions of the western side of the warm ring could not be determined.

Figure 3.2.3.2 is the salinity analysis for Transect I. After Station 11 along I, the recorder arm for the STD's salinometer became inoperable, and only the salinity analysis given in Figure 3.2.3.2 were available for the entire period the R/V ADVANCE II was at sea.

The values of salinity were higher than those normally observed in this region at this time of year. Calibration of the STD's salinometer was accomplished before and after the case study, and the data were corrected based on these calibrations. Even so, they remained high. Though the values are suspect, the relative variation of salinity is believed to be good.

Below 200 m, the data indicates that the eddy is also made up a dome of less saline water (Stumpf et al., 1973). Above 200 m, the salinity is uniform except near the surface. The value of the salinity in the eddy above 200 m is only slightly lower than that in the Sargasso Sea and in the high salinity core of the Gulf Stream which suggests that there has been considerable mixing in this layer since the genesis of the eddy.

The warm ring has a shallow layer (25-to 50-m deep) of lower salinity water than the surrounding water at the same level; however, the salinity in the surface layer of the warm ring appears to be identical to that found in the surface layer in the middle of the cold eddy. The eastern extension of the warm ring is less saline than the western side.

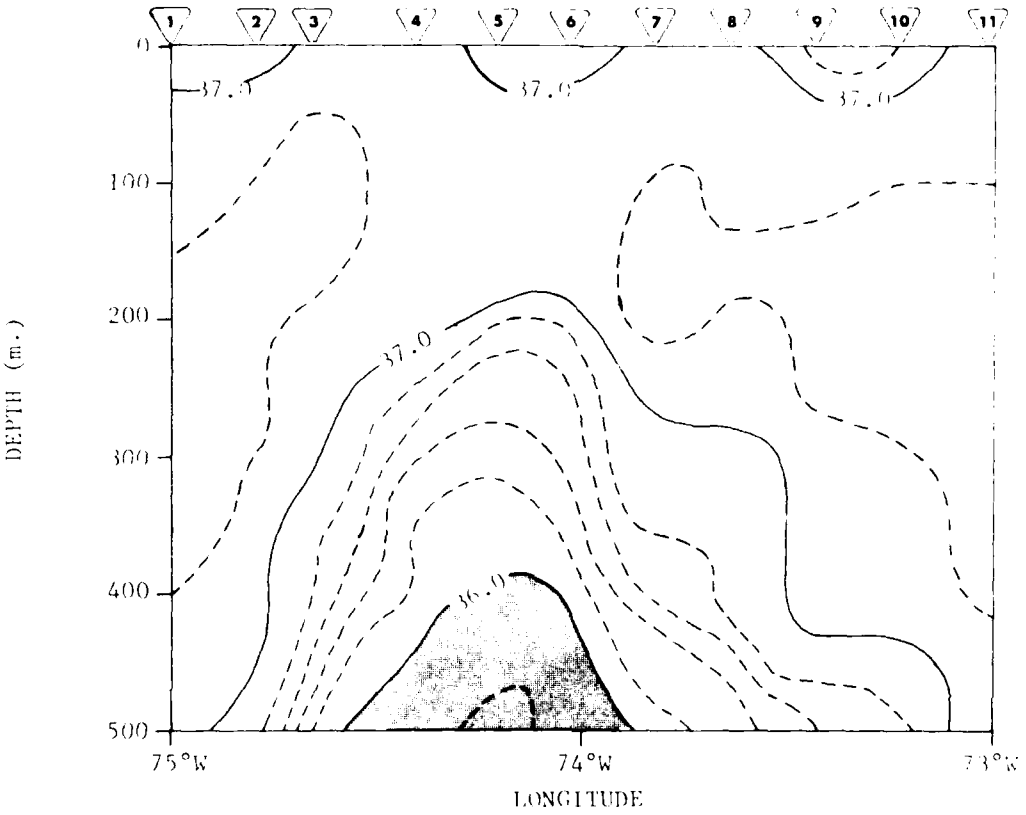

Figure 3.2.3.2 Vertical salinity (°/₀₀) cross-section along Transect I. The integration period was 0230-2300 EDT, 27 March. Station numbers are given at the top of the figure.

According to the VHRR analyses in Figure 3.2.2.2, Transect II passed through the southern tip of the cold eddy. The temperature analysis using the data collected at stations along Transect II is given in Figure 3.2.3.3. The integration period for the analysis was 0310 EDT, 28 March 1974 to 0240 EDT, 29 March 1974. Below 200 m, the analyses shows a weak dome of cold water. The coldest water at 500 m has a temperature of 14.4°C, and the center of cold water is shifted eastward reflecting the northwest-southeast horizontal orientation of the cold eddy discussed previously. Above 200 m, the region of uniform temperature evident in the previous analyses (Figure 3.2.3.1) is not a part of the physical structure of the cold eddy in this analysis. The most comparable feature is the region of weak temperature gradient between the 100-m and 200-m levels around 74°W.

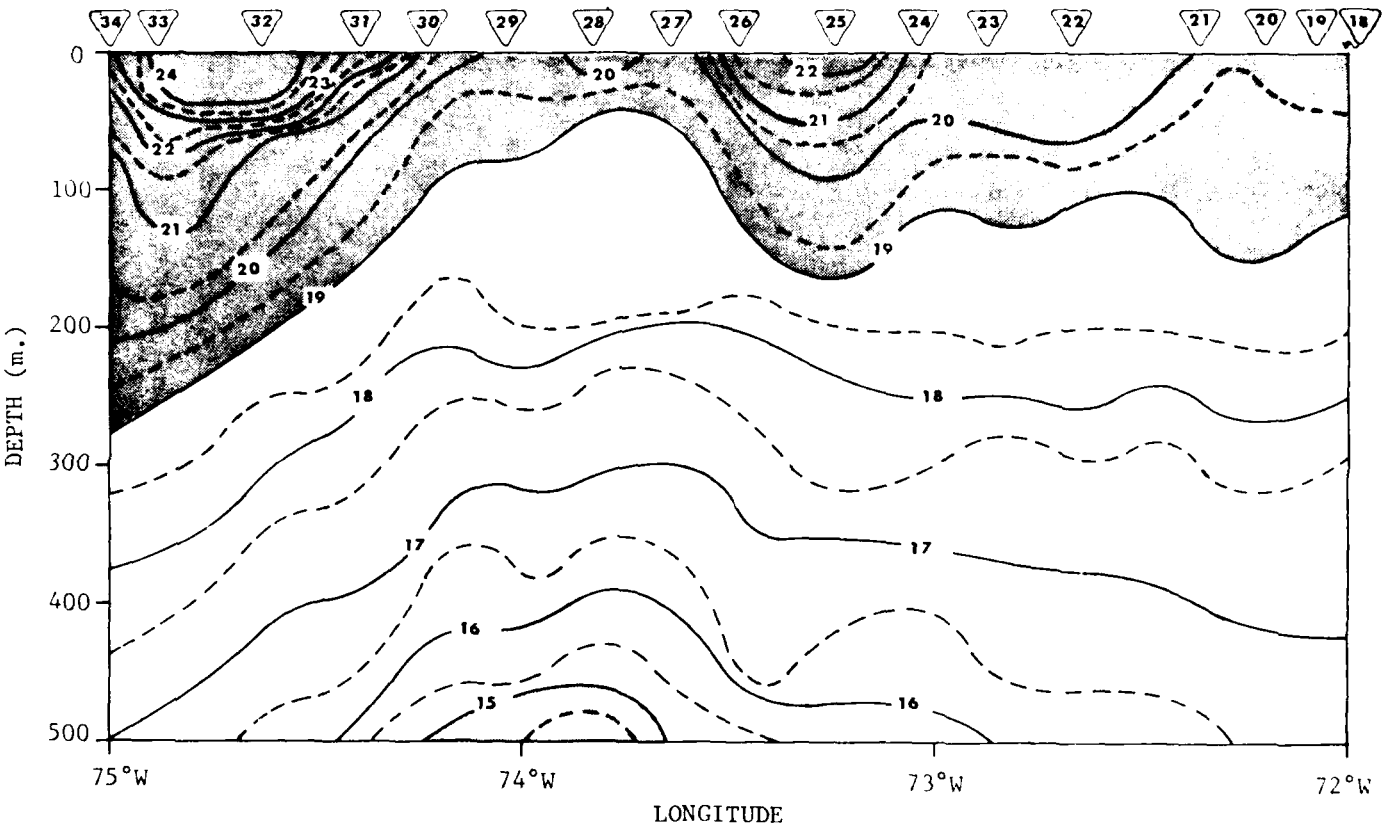

Figure 3.2.3.3 Vertical temperature (°C) cross-section along Transect II. The integration period was 0310 EDT 28 March 1974 to 0240 EDT, 29 March 1974. Station numbers are given at the top of the figure.

Both the east and west sides of the warm ring are evident in this analysis also, but the surface water on the western side (24.0°C) is warmer than that on the eastern side (22.4°C). The 7 March, NOAA-2 VHRR analyses (Figure 3.2.2.1) suggests the possibility that the western portion of the warm ring along Transect II is warmer (≈ 24°C) than the eastern part (≈ 22°C); but no such indications are evident on the 1 April NOAA-3 analyses in this region (Figure 3.2.2.1). The temperature differences between the east and west side of the warm ring may be a result of mixing of this apparent Gulf Stream water with Sargasso Sea water as it circulates around the cold eddy. The warm ring appears to be narrower on the east side (60-km wide) than on the west side (at least 120-km wide). According to the 19°C isotherm, it also appears to extend to greater depths on the west side (280 m) than on the east side (about 180 m).

According to the satellite data, Transect III should have passed through the heart of the eddy. However, comparison of the temperature data from Transect III (Figure 3.2.3.4) with that from Transect I (Figure 3.2.3.1) indicates that the actual center of the cold eddy must have been nearer to that found using data from Transect I since the lowest temperature at 500 m along Transect III is 12.4°C, a degree centigrade higher than that found along Transect I. The dome of cold water characterizing the lower portion of the cold eddy extends nearer to the surface (about the 100-m level) in this analysis than in any of the other analyses. This factor is a result of what appears to be a secondary perturbation on the cold eddy centered about 110 km away from the initial station of Transect III and found above the 300-m level. Figure 3.2.3.5 shows that the horizontal manifestation of this perturbation at the 150-m level is found in the same location as the surface cold lens in the cold eddy identified using the 1 April NOAA data. This suggests the possibility that the cooling of the surface water in the central regions of the eddy between 7 March and 1 April may be a result of bringing cooler subsurface water to the surface either by mixing or by upwelling rather than an artifact of the satellite sensors.

According to Figure 3.2.3.4, only the western side of the warm ring is evident in the cross section because Transect II did not extend far enough. The structure of the warm ring on the western side is similar

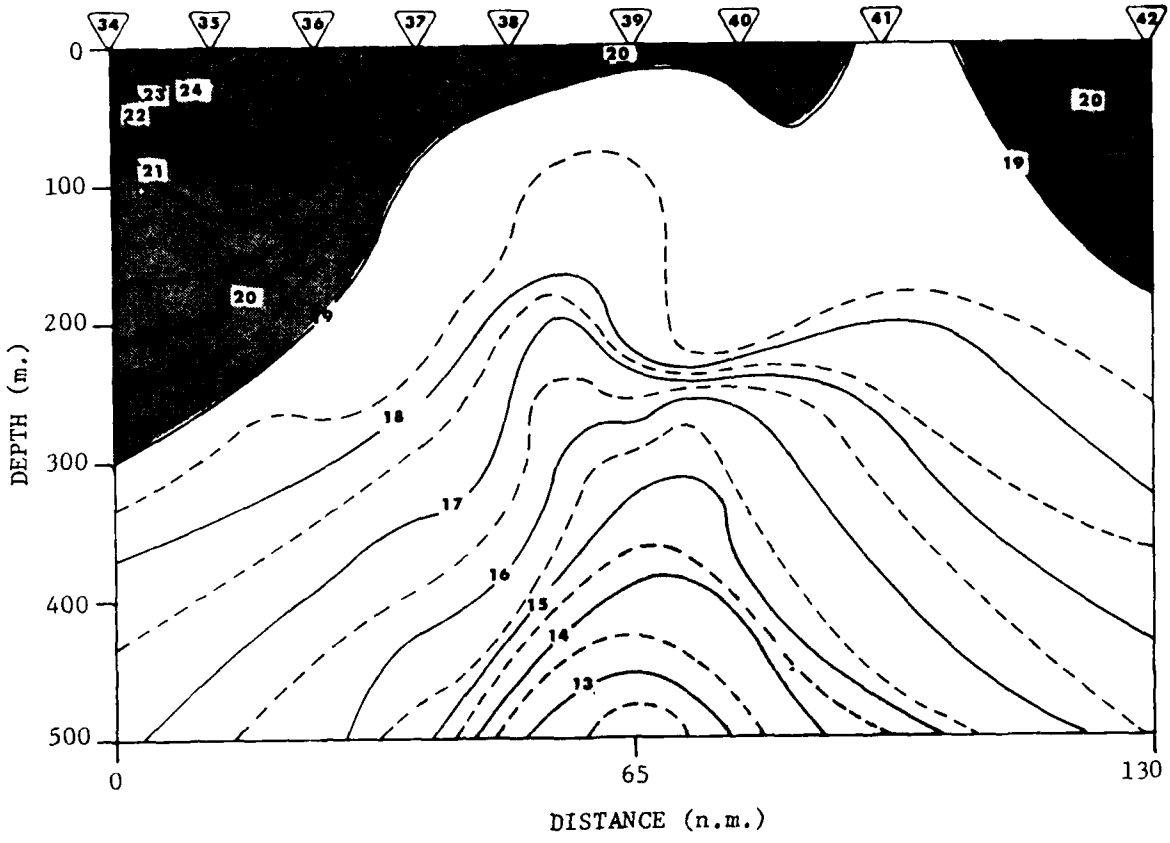

32° 25'N
75° 00'W

32° 36'N
73° 59'W

33° 00'N
72° 52'W

Figure 3.2.3.4 Vertical temperature (°C) cross-section along Transect III. The integration period was 0240-1115 EDT, 29 March 1974. Station numbers are given at the top of the Figure.

to that found along Transect II. The highest temperature is 24.0°C; the width is about 120 km; and it extends to about the 300-m level.

3.2.4 Estimates of the Circulation in the Cold Eddy

During the course of the field program, there was an attempt to obtain data on the near-surface circulation of the cold eddy. A free-drifting EOLE buoy was released in the warm ring of the cold eddy. The drag fins of the buoy were set at approximately the 4-m level so that the data obtained would characterize the properties of the near-surface circulation. The buoy was released on 27 March 1974 and retrieved on 23 April 1974 (a 28-day period). The position of the buoy was to be determined by data collected by the EOLE satellite (Morel and Bandeen, 1973). Unfortunately,

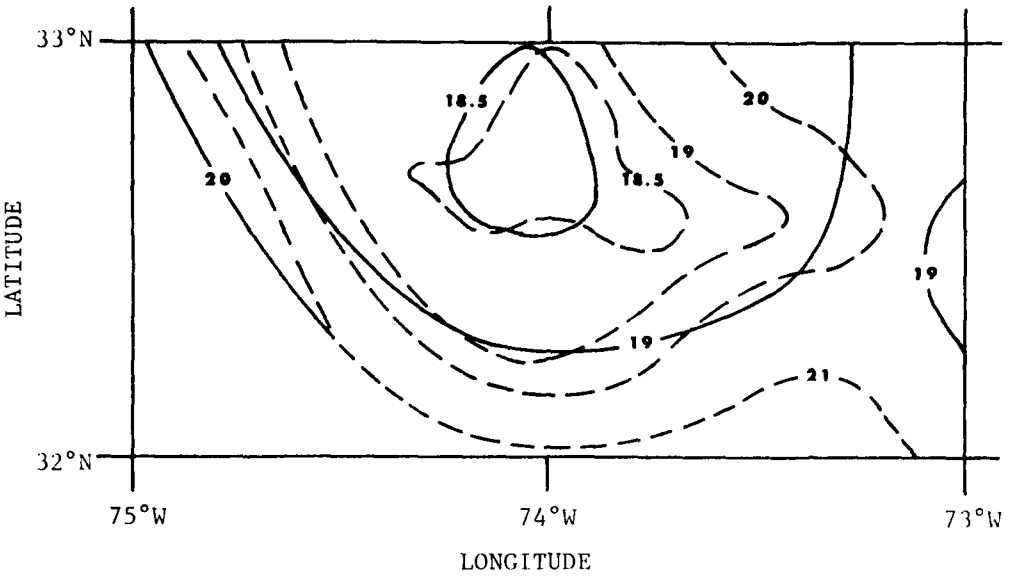

Figure 3.2.3.5 Comparison of the horizontal temperature (°C) structure at the 150-m level (solid line) with that at the surface (dashed line) in the cold eddy. The 150-m temperature analyses were made using the R/V ADVANCE II data and the surface analysis, the 1 April NOAA-3 data.

mechanical problems were encountered aboard the EOLE satellite during this period and no data was retrieved. However, three position fixes for the buoy were available from ship and aircraft data. These data are given in Figure 3.2.4.1, along with the date of the observation. These data were

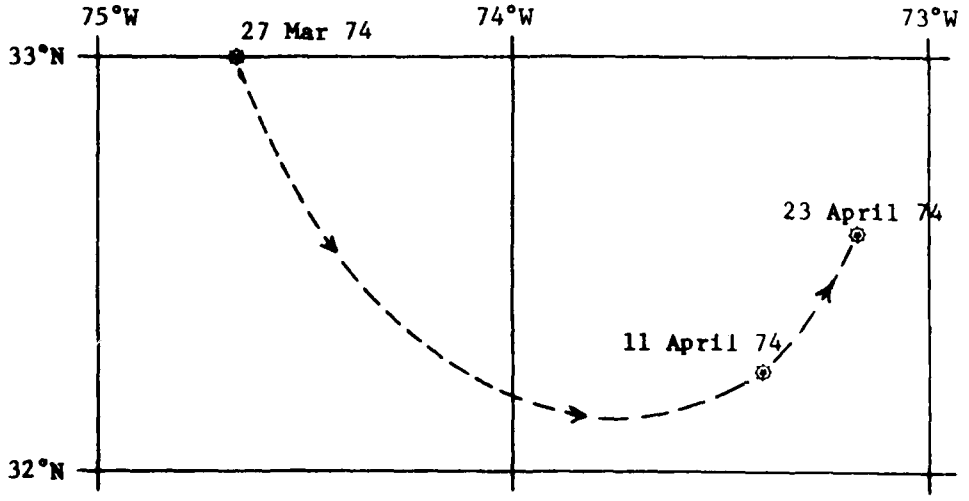

Figure 3.2.4.1 Plot of the position of the free-drifting buoy as determined by ship and aircraft, and hypothetical trajectory (dashed line) of buoy as determined by the buoy position data and the sea-surface temperature data. The period is 27 March 1974 to 23 April 1974.

combined with the 1 April, VHRR sea-surface temperature analysis (Figure 3.2.2.2) to produce the hypothetical trajectory (the dashed line in the figure) of the buoy. The hypothetical trajectory was constructed assuming that buoy is on its first revolution around the eddy. The possibility exists that buoy made more than one revolution around the eddy and the buoy locations represent positions on different revolutions. (For instance, if the actual surface current in the eddy is 1 ms^{-1}, the buoy would have made 3.5 revolutions in the 27-day period).

The data indicate that there is cyclonic curvature to the flow. It appears from the position of the buoy and the elapsed time that the currents in the warm ring are stronger on the western side. The estimated near-surface current speed on the western side based on the hypothetical trajectory and elapsed time was 15 cm s^{-1} and that on the eastern side was 5 cm s^{-1}.

Some of the above evaluations were corraborated by the analysis of the geostrophic current. The geostrophic current was calculated using the temperature and salinity data gathered along Transect I. The computations were made relative to the surface. For this reason, only the qualitative aspects should be considered of any importance. The analysis (Figure 3.2.4.2) suggested that there are southward currents on the west side and northward currents on the east sided indicative of cyclonic flow. It further suggested that the currents on the west side are stronger than on the east side, and that the maximum current is most probably below the 500-m level on either side of the eddy.

3.2.5 Time Changes in the Structure of the Cold Eddy

Figure 3.2.5.1 yields two temperature profiles obtained in the approximate center of the cold eddy. The 28 November 1973 data were obtained by the R/V KNORR, and the 28 March 1974 data by the R/V ADVANCE II. All available evidence indicated that these profiles were in the same eddy. It is obvious from these data that marked changes in the cold eddy had taken place in the intervening period between observations. The thermocline lowered 85 m in the period, and strength of the thermocline decreased (i.e., the lapse rate of temperature between the top of the thermocline and 100 m below that level was 7.5°C/100 m on 28 November and was 3.75°C/100 m on 27 March).

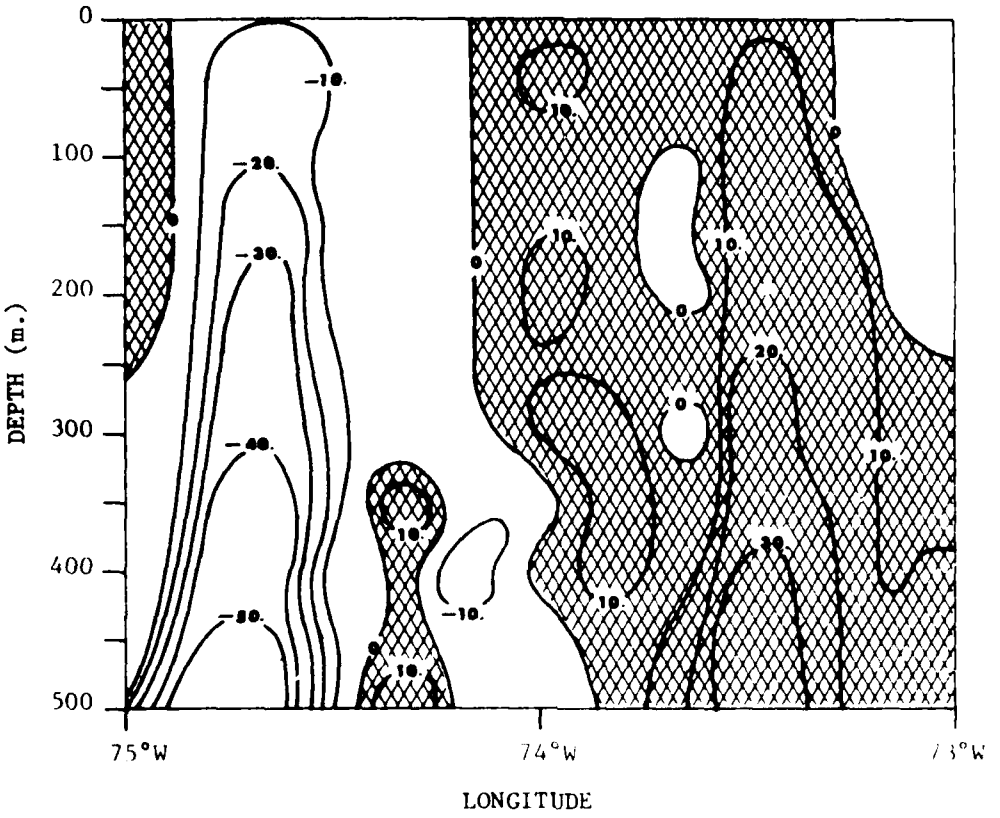

Figure 3.2.4.2 Analysis of geostrophic current (cm/s) along Transect I made using the temperature and salinity data from that transect.

An extremely important aspect is the change in the available potential energy of the cold eddy over the period. The change in available potential energy was determined in the following manner. According to Lorenz (1957), the available potential energy, A, is given by

$$A = \frac{1}{2} \int_p - \frac{(T'^2)}{\bar{T}(\Gamma_d - \bar{\Gamma})} dp \quad ,$$

where p is pressure, $\bar{T}$ is the isobaric temperature in the reference state, $\bar{\Gamma}$ is the lapse rate of temperature in the reference state, Γ_d is the adiabatic lapse rate, and T' is the departure of the existing isobaric temperature from that of the reference state. The rate change in available potential temperature is derived by taking the local derivative of the

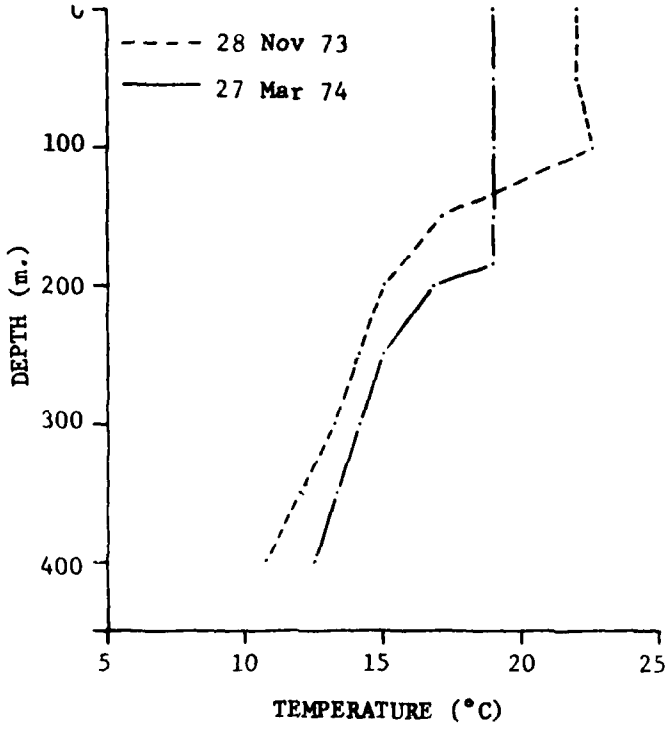

Figure 3.2.5.1 Temperature profile in cold eddy on 28 November 1973 (dashed line) and on 27 March 1974 (solid line).

above expression; i.e.,

$$\frac{\partial A}{\partial t} = \frac{1}{2} \int_p \frac{(T'^2)}{\bar{T}(\Gamma_d - \bar{\Gamma})} \frac{\partial}{\partial t} \ln(T'^2)\, dp.$$

Replacing $\frac{\partial}{\partial t} \ln(T'^2)$ by its pressure-averaged value, $\frac{\partial}{\partial t} \ln(\tau'^2)$, then

$$\frac{\partial A}{\partial t} \approx A \frac{\partial}{\partial t} \ln(\tau'^2) \quad ,$$

or

$$\frac{\partial}{\partial t} \ln A \approx \frac{\partial}{\partial t} \ln (\tau'^2) \quad .$$

Integration yields

$$\frac{A_e}{A_i} \approx \frac{\tau_e'^2}{\tau_i'^2} \qquad 3.2.5.1$$

where the subscript e refers to the end of the period and i refers to the initial time.

Equation 3.2.5.1 was evaluated using the data presented in Figure 3.2.5.1. Average temperature data for the region of interest were used for the reference state. The results of the calculation is

$$\left(\frac{A_e}{A_i}\right)_{\substack{\text{cold} \\ \text{eddy}}} = 0.66 \quad ;$$

that is, there was a 34% decrease in available potential energy in the first 400 m of the eddy between 28 November 1973 and 27 March 1974. The energy dissipation is most likely a result of heat dispersion and conversion of potential energy into kinetic energy.

3.2.6 Conclusions

A cold eddy whose genesis was in late August 1973 was studied. The study period commenced in March 1974. It was shown that below 200 m, the eddy is a very pronounced dome of cold, relatively fresh water. Above 200 m, the eddy has a uniform temperature and salinity, both vertically and horizontally. The 1 April 1974, VHRR sea-surface temperature data indicate the possibility that the surface temperature decreased by about 0.5°C in the central region of the eddy over an area of about 2800 km^2. The area of the eddy on the above date was about 9000 km^2, so that the temperature decrease occurred over about 30% of the eddy at the surface. The data collected by the R/V ADVANCE II along Transect III on 29 March 1974, suggested that the temperature decrease may possibly be due to mixing or upwelling. However, there is the strong possibility that the cooling is due to the sensor degradation on NOAA-2. Temperature decreases are unexpected in the eddy since it is believed that the cold eddy is dissipating which normally would be accompanied by a temperature increase in the central core. The fact that the eddy is dissipating was substantiated

1) by calculations that showed that the available potential energy of the cold eddy decreased by 34% in a four-month period, and 2) by demonstrating that the thermocline in the cold eddy lowered and weakened in the same four months.

The warm ring, which is considered an integral part of the structure of the cold eddy, was about 60- to 120-km wide and extended down to about the 100- to 300-m level. The data indicated that the salinity in the warm ring was less than or equal to that in the central region of the cold eddy. This was attributed to the fact that mixing in the central regions of the eddy with the Sargasso Sea water and the water in the high salinity core of the Gulf Stream had substantially increased the salinity in the eddy, and that the near-surface Gulf Stream water is less saline than either the Sargasso Sea water or the Gulf Stream's high salinity core.

The isotherm pattern in the VHRR sea-surface temperature analyses suggested that the circulation of the eddy was entraining Gulf Stream water into the warm ring. Available evidence, the isotherm pattern in the VHRR sea-surface temperature analysis, free-drifting buoy position data, and geostrophic computation, confirm a cyclonic circulation in the eddy. These data further suggest that the current speeds were greater on the west side of the eddy than on the east side. The geostrophic computations suggest that the maximum current speed is found below the 500-m level.

SECTION 4

CONCLUSION

The results of this study has demonstrated that the NOAA satellite data may be used in oceanographic research (1) to locate significant oceanic perturbations and (2) to aid in the study of the structure of perturbations by integrating in-situ data with the satellite infrared data. Probably, the most significant contribution of the satellite infrared data to the analysis of the perturbation was the capability of these data to yield an instantaneous, near-synoptic view of the sea-surface temperature pattern which in many cases brought to light features that could not have been established by the in-situ data alone, except through an expensive and intensive field program.

REFERENCES

Barrett, J. R., "Available potential energy of Gulf Stream rings", Deep-Sea Res., 18, 1221-1231, 1971.

DeRycke, R. J. and Rao, P. K., "Eddies along a Gulf Stream boundary viewed from a very high resolution radiometer", 3: 4, 490-492, 1973.

Ewing, G. and E. D. McAllister, "On the thermal boundary layer of the ocean", Science, 131: 1374-1376, 1960.

Maul, G. A. and D. V. Hansen, "An observation of the Gulf Stream front structure by ship, aircraft and satellite", Remote Sensing of the Environment, 2, 109-116, 1972.

Morel, P. and W. Bandeen, "The EOLE Experiment: Early results and current objectives", Bulletin of the American Meteorological Society, 54: 4, 298-306, 1973.

Parker, C. E., "Gulf Stream rings in the Sargasso Sea", Deep-Sea Res., 18, 981-903, 1971.

Rao, P. K., A. E. Strong and R. Koffler, "Gulf Stream meanders and eddies as seen in satellite infrared imagery", J. Phys. Ocean., 3, 238-239, 1971.

Richardson, P. L., A. E. Strong and J. A. Knauss, "Gulf Stream eddies: Recent observations in the Western Sargasso Sea", J. Phys. Ocean., 3: 3, 297-301, 1973.

Smith, W. L., P. K. Rao, K. Koffler, and W. R. Curtis, "The determination of sea-surface temperatures from satellite high resolution infrared window radiation measurements", Mon. Wea. Rev., 98: 8, 607-611, 1970.

Stommel, H., "The Gulf Stream", Univ. Cal. Press, 248, 1965.

Stumpf, H. G., A. E. Strong and J. Pritchard, "Large cyclonic eddies of the Sargasso Sea", 17: 4, 208-210, 1973.

Vukovich, F. M., "Detailed sea-surface temperature analysis utilizing NIMBUS HRIR data", Mon. Wea. Rev., 99: 11, 812-817, 1971.

Vukovich, F. M., "Synoptic scale air-sea interaction study using NOAA-1 SRIR data", Final Report, NOAA Contract No. 2-35184, Research Triangle Institute, Research Triangle Park, N. C., 85 pp., 1972.

Vukovich, F. M., "The detection of near-shore eddy motion and wind-driven using NOAA-1 sea-surface temperature data", J. Geophys. Res., 79: 6, 853-860, 1974.

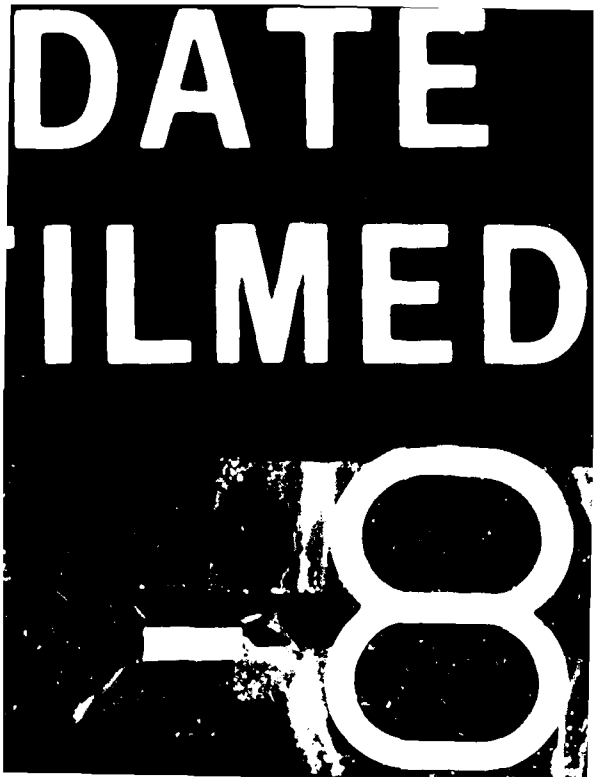
DATE
ILMED
-8